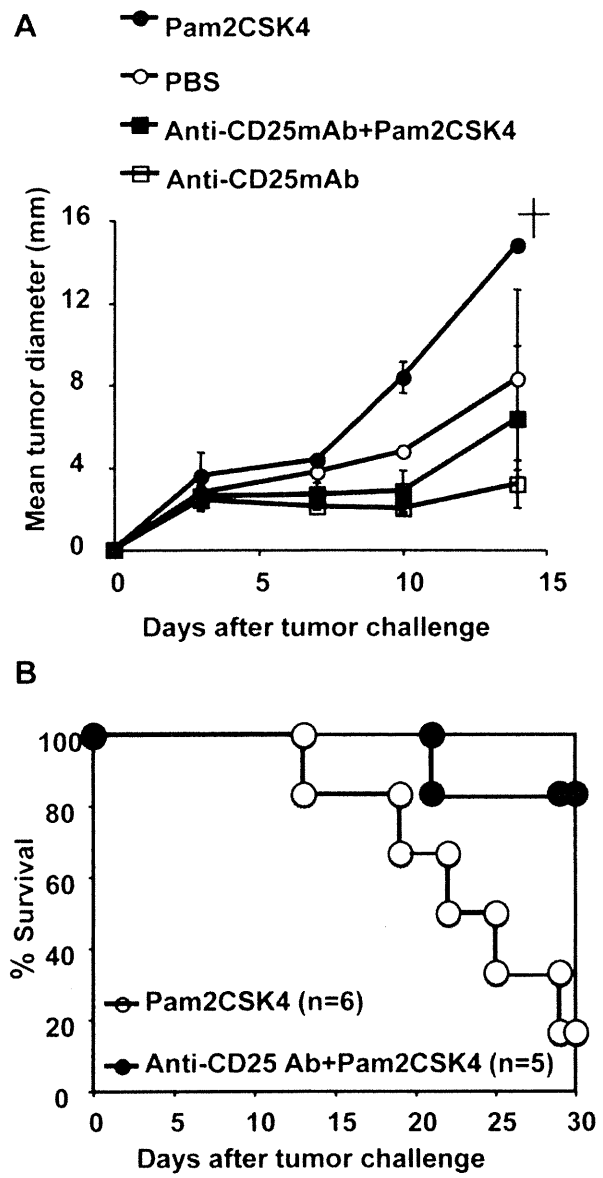

Figure 5. NK-sensitive tumors grow slowly when Pam2CSK4 is injected into T reg-depleted mice. (A) B6 mice were i.p. injected with 500 μg of anti-CD25mAb (PC61) on day -3. The mice were injected with B16D8 melanoma cells (2×10^5) into their back on day 0. Pam2CSK4 (10 nmol) or PBS was injected twice a week from day 0 to day 14. Tumor growth was monitored twice a week. n = 3 for each group. A cross indicates the death of one mouse. One representative experiments from two similar experiments is shown. (B) As in (A), but the survival curve summarized from two separate experiments is shown.
doi:10.1371/journal.pone.0018833.g005

experiments used mice that were between 6–12 weeks-of-age at the time of first procedure. All mice were used according to the guidelines of the institutional animal care and use committee of the Hokkaido University, who approved this study as ID number: 08-0243, " Analysis of immune modulation by toll-like receptors".

Antibodies and reagents

PE-conjugated CD25 (PC61), Alexa-488 conjugated anti-CD25 (7D4), FITC or APC conjugated CD4 (RM4-5), CD11c, NK1.1, purified anti-CD16/CD32 (2.4G2), purified anti-CD3 (2C11), and isotype antibodies were obtained from Biolegend (San Diego, CA, USA). Anti-CD11c, anti-NK and streptavidin microbeads were purchased from Miltenyi Biotec (Gladbach, Germany). Carboxy-fluorescein diacetate succinimidyl ester (CFSE) and TOPRO-3 were from Molecular Probes (Eugene, OR, USA). The anti-mouse Foxp3 (FJK-16s) staining kit was from eBioscience (San Diego, CA, USA). Purified anti-CD25 (PC61) mAb was a gift from Dr. Ralph Steinman (The Rockefeller University, NY, USA) and anti-CD25 hybridoma cells were from Dr. Jun Shimizu (Kyoto University, Kyoto, Japan). Some of the anti-CD25 (PC61) mAb was produced in CB17SCID mice in our animal facility and purified by ammonium sulfate precipitation. Purified anti-IL-10 mAb (JES5-2A5) was prepared as described previously [54]. Pam2CSK4, Pam2CSK2 and MALP2 short lipopeptides were synthesized by Biologica Co. Ltd (Nagoya, Japan). Pam2-#6 and Pam2-#12 were from Dr. Yukari Fujimoto and Dr. Koichi Fukase (Osaka University, Osaka, Japan).

Cell isolations

$CD4^+$ T cells were first negatively separated by MACS beads from lymph nodes and spleen cell suspensions (>90%) (Miltenyi Biotech) and T reg cells were further purified by a FACS Aria II (BD Bioscience, Franklin Lakes, NJ, USA). Spleen $CD11c^+$ DCs were selected with anti-CD11c beads (Miltenyi Biotech). Bone marrow DCs (BM-DCs) were cultured with GM-CSF as previously described [22]. NK cells were purified from spleen by anti-NK beads (Miltenyi Biotech). To analyze the activation of DCs and NK cells *in vivo* by Pam2 lipopeptides, 10 nmol of Pam2 lipopeptides was subcutaneously (s.c.) or intraperitoneally (i.p.) and 12–16 hours later, the spleen was analyzed by flow cytometry. Both routes of injection gave similar results.

Measuring cytokine production

DCs or NK cells were stimulated with 100 nM of Pam2 lipopeptides for 24 hours and the supernatants were measured for IL-10 by ELISA (eBiosciences). $CD4^+$ T cells from OT II transgenic mice were cultured with spleen DCs with or without 100 nM of Pam lipopeptides at the various doses of OVA peptide for five days. The supernatants were measured for IL-10 by ELISA. Serum from Pam2 lipopeptides treated mice or control mice were taken one day after i.p. injection and were measured for IL-10, INF-c, IL-4 and IL-17 by Cytometric Bead Array (BD Bioscience). Analysis with the Cytometric Bead Array was performed according to the manufacturer's instructions.

Quantitative PCR

Total RNA was isolated with TRIzol (Invitrogen by life technologies, Carlsbad, CA, USA), and reversed transcribed by High Capacity cDNA Transcription Kit (ABI by life technologies, Carlsbad, CA, USA) according to manufacturer instructions. The qPCR was performed with the Step One Real-Time PCR system (ABI). The primers used for real-time PCR have been reported previously [29].

In vivo tumor challenge

Mice were s.c. injected with $2-3\times10^5$ B16D8 cells into the back. B16D8 melanoma is a NK-sensitive B16 melanoma cell line, which we have previously established [22]. The tumor growth was monitored twice a week. Sometimes mice were pre-treated with

500 μg of anti-CD25 mAb three days before tumor challenge. Then, 10 nmol of Pam2 lipopeptides or control saline was s.c injected into footpad or i.p. injected twice a week. The both routes of injection gave similar results.

In vitro suppression assay using T reg cells

The classical *in vitro* suppression assay was performed as previously described [32,55]. Briefly, $CD25^+CD4^+$ T cells were purified by flow cytometry and used as suppressor cells. CFSE-labeled $CD25^-$ $CD4^+$ T cells or $CD4^+$ T cells were stimulated with or without anti-CD3 mAb (2C11) and 15–20 Gy irradiated spleen cells. Various numbers of suppressor cells were added to the culture. After three day culture, cells were stained with CD4 –PE and dead cells were gated out with TOPRO-3 (Molecular Probes). All cells in each culture were acquired using the FACS calibur (BD Bioscience) to have the cell yield and number of live $CFSE^+$ cells/culture was calculated. Analysis was performed with Flowjo software (TreeStar, USA).

Supporting Information

Figure S1 NK cells up-regulates CD69 after systemic injection of Pam2 lipopeptides. Mice were subcutaneously injected with the indicated Pam2 lipopeptides (10 nmol) or saline. After 16 hours, splenic NK cells were analyzed by flow cytometry. Plots were gated on $NK1.1^+$ cells.
(TIF)

Figure S2 The frequency of T reg cells returns to normal at day 7 after systemic injection of Pam2 lipopeptides. WT mice were i.p. injected with Pam2CSK4 (10 nmol). After seven days, spleen (Sp) and lymph node (LN) cells were analyzed for the expression of Foxp3. The plots were gated on $CD4^+$ T cells. One of two experiments is shown for the FACS plots.
(TIF)

Acknowledgments

We thank Ms. Ryoko Sawahata for technical assistance at the beginning of the project, Dr. Hussein Aly for reading the manuscript, Dr. Kazuya Iwabuchi and Dr. Shizuo Akira for the mice, Dr. Yukari Fujimoto and Dr. Koichi Fukase for the peptides, Dr. Jun Shimizu for providing the hybridoma cells and Dr. Ralph Steinman for providing the antibody.

Author Contributions

Conceived and designed the experiments: SY MM TS. Performed the experiments: SY KO AM. Analyzed the data: SY KO. Contributed reagents/materials/analysis tools: HY. Wrote the paper: SY TS.

References

1. Nishikawa H, Sakaguchi S (2010) Regulatory T cells in tumor immunity. Int J Cancer 127: 759–767.
2. Curiel TJ (2008) Regulatory T cells and treatment of cancer. Curr Opin Immunol 20: 241–246.
3. Ko K, Yamazaki S, Nakamura K, Nishioka T, Hirota K, et al. (2005) Treatment of advanced tumors with agonistic anti-GITR mAb and its effects on tumor-infiltrating Foxp3+CD25+CD4+ regulatory T cells. J Exp Med 202: 885–891.
4. Li X, Kostareli E, Suffner J, Garbi N, Hammerling GJ (2010) Efficient Treg depletion induces T-cell infiltration and rejection of large tumors. Eur J Immunol 40: 3325–3335.
5. Curiel TJ, Coukos G, Zou L, Alvarez X, Cheng P, et al. (2004) Specific recruitment of regulatory T cells in ovarian carcinoma fosters immune privilege and predicts reduced survival. Nat Med 10: 942–949.
6. Ghiringhelli F, Puig PE, Roux S, Parcellier A, Schmitt E, et al. (2005) Tumor cells convert immature myeloid dendritic cells into TGF-beta-secreting cells inducing CD4+CD25+ regulatory T cell proliferation. J Exp Med 202: 919–929.
7. Shimizu J, Yamazaki S, Sakaguchi S (1999) Induction of tumor immunity by removing CD25+CD4+ T cells: a common basis between tumor immunity and autoimmunity. J Immunol 163: 5211–5218.
8. Onizuka S, Tawara I, Shimizu J, Sakaguchi S, Fujita T, et al. (1999) Tumor rejection by *in vivo* administration of anti-CD25 (interleukin-2 receptor alpha) monoclonal antibody. Cancer Res 59: 3128–3133.
9. Teng MW, Swann JB, von Scheidt B, Sharkey J, Zerafa N, et al. (2010) Multiple antitumor mechanisms downstream of prophylactic regulatory T-cell depletion. Cancer Res 70: 2665–2674.
10. Sutmuller RP, van Duivenvoorde LM, van Elsas A, Schumacher TN, Wildenberg ME, et al. (2001) Synergism of cytotoxic T lymphocyte-associated antigen 4 blockade and depletion of CD25+ regulatory T cells in antitumor therapy reveals alternative pathways for suppression of autoreactive cytotoxic T lymphocyte responses. J Exp Med 194: 823–832.
11. Quezada SA, Peggs KS, Curran MA, Allison JP (2006) CTLA4 blockade and GM-CSF combination immunotherapy alters the intratumor balance of effector and regulatory T cells. J Clin Invest 116: 1935–1945.
12. Peggs KS, Quezada SA, Chambers CA, Korman AJ, Allison JP (2009) Blockade of CTLA-4 on both effector and regulatory T cell compartments contributes to the antitumor activity of anti-CTLA-4 antibodies. J Exp Med 206: 1717–1725.
13. Klages K, Mayer CT, Lahl K, Loddenkemper C, Teng MW, et al. (2010) Selective depletion of Foxp3+ regulatory T cells improves effective therapeutic vaccination against established melanoma. Cancer Res 70: 7788–7799.
14. Steinman RM, Banchereau J (2007) Taking dendritic cells into medicine. Nature 449: 419–426.
15. Steinman RM, Nussenzweig MC (2002) Avoiding horror autotoxicus: the importance of dendritic cells in peripheral T cell tolerance. Proc Natl Acad Sci U S A 99: 351–358.
16. Dubensky TW, Jr., Reed SG (2010) Adjuvants for cancer vaccines. Semin Immunol 22: 155–161.
17. Seya T, Matsumoto M (2009) The extrinsic RNA-sensing pathway for adjuvant immunotherapy of cancer. Cancer Immunol Immunother 58: 1175–1184.
18. Yamazaki S, Iyoda T, Tarbell K, Olson K, Velinzon K, et al. (2003) Direct expansion of functional CD25+ CD4+ regulatory T cells by antigen-processing dendritic cells. J Exp Med 198: 235–247.
19. Yamazaki S, Patel M, Harper A, Bonito A, Fukuyama H, et al. (2006) Effective expansion of alloantigen-specific Foxp3+ CD25+ CD4+ regulatory T cells by dendritic cells during the mixed leukocyte reaction. Proc Natl Acad Sci U S A 103: 2758–2763.
20. Tsuji S, Matsumoto M, Takeuchi O, Akira S, Azuma I, et al. (2000) Maturation of human dendritic cells by cell wall skeleton of Mycobacterium bovis bacillus Calmette-Guerin: involvement of toll-like receptors. Infect Immun 68: 6883–6890.
21. Azuma I, Seya T (2001) Development of immunoadjuvants for immunotherapy of cancer. Int Immunopharmacol 1: 1249–1259.
22. Akazawa T, Ebihara T, Okuno M, Okuda Y, Shingai M, et al. (2007) Antitumor NK activation induced by the Toll-like receptor 3-TICAM-1 (TRIF) pathway in myeloid dendritic cells. Proc Natl Acad Sci U S A 104: 252–257.
23. Uehori J, Matsumoto M, Tsuji S, Akazawa T, Takeuchi O, et al. (2003) Simultaneous blocking of human Toll-like receptors 2 and 4 suppresses myeloid dendritic cell activation induced by Mycobacterium bovis bacillus Calmette-Guerin peptidoglycan. Infect Immun 71: 4238–4249.
24. Murata M (2008) Activation of Toll-like receptor 2 by a novel preparation of cell wall skeleton from Mycobacterium bovis BCG Tokyo (SMP-105) sufficiently enhances immune responses against tumors. Cancer Sci 99: 1435–1440.
25. Azuma M, Sawahata R, Akao Y, Ebihara T, Yamazaki S, et al. (2010) The peptide sequence of diacyl lipopeptides determines dendritic cell TLR2-mediated NK activation. PLoS One 5: e12550.
26. Akazawa T, Inoue N, Shime H, Kodama K, Matsumoto M, et al. (2010) Adjuvant engineering for cancer immunotherapy: Development of a synthetic TLR2 ligand with increased cell adhesion. Cancer Sci 101: 1596–1603.
27. Sun CM, Hall JA, Blank RB, Bouladoux N, Oukka M, et al. (2007) Small intestine lamina propria dendritic cells promote de novo generation of Foxp3 T reg cells via retinoic acid. J Exp Med 204: 1775–1785.
28. Coombes JL, Siddiqui KR, Arancibia-Carcamo CV, Hall J, Sun CM, et al. (2007) A functionally specialized population of mucosal CD103+ DCs induces Foxp3+ regulatory T cells via a TGF-beta and retinoic acid-dependent mechanism. J Exp Med 204: 1757–1764.
29. Manicassamy S, Ravindran R, Deng J, Oluoch H, Denning TL, et al. (2009) Toll-like receptor 2-dependent induction of vitamin A-metabolizing enzymes in dendritic cells promotes T regulatory responses and inhibits autoimmunity. Nat Med 15: 401–409.
30. Collison LW, Pillai MR, Chaturvedi V, Vignali DA (2009) Regulatory T cell suppression is potentiated by target T cells in a cell contact, IL-35- and IL-10-dependent manner. J Immunol 182: 6121–6128.
31. Murai M, Turovskaya O, Kim G, Madan R, Karp CL, et al. (2009) Interleukin 10 acts on regulatory T cells to maintain expression of the transcription factor Foxp3 and suppressive function in mice with colitis. Nat Immunol 10: 1178–1184.
32. Yamazaki S, Bonito AJ, Spisek R, Dhodapkar M, Inaba K, et al. (2007) Dendritic cells are specialized accessory cells along with TGF-b for the

differentiation of Foxp3+ CD4+ regulatory T cells from peripheral Foxp3- precursors. Blood 110: 4293–4302.
33. Roncarolo MG, Gregori S, Battaglia M, Bacchetta R, Fleischhauer K, et al. (2006) Interleukin-10-secreting type 1 regulatory T cells in rodents and humans. Immunol Rev 212: 28–50.
34. Asseman C, Mauze S, Leach MW, Coffman RL, Powrie F (1999) An essential role for interleukin 10 in the function of regulatory T cells that inhibit intestinal inflammation. J Exp Med 190: 995–1004.
35. Rubtsov YP, Rasmussen JP, Chi EY, Fontenot J, Castelli L, et al. (2008) Regulatory T cell-derived interleukin-10 limits inflammation at environmental interfaces. Immunity 28: 546–558.
36. Aumeunier A, Grela F, Ramadan A, Pham Van L, Bardel E, et al. (2010) Systemic Toll-like receptor stimulation suppresses experimental allergic asthma and autoimmune diabetes in NOD mice. PLoS One 5: e11484.
37. Chen Q, Davidson TS, Huter EN, Shevach EM (2009) Engagement of TLR2 does not reverse the suppressor function of mouse regulatory T cells, but promotes their survival. J Immunol 183: 4458–4466.
38. Brooks MN, Rajaram MV, Azad AK, Amer AO, Valdivia-Arenas MA, et al. (2010) NOD2 controls the nature of the inflammatory response and subsequent fate of Mycobacterium tuberculosis and M. bovis BCG in human macrophages. Cell Microbiol 13: 402–418.
39. Ghiringhelli F, Menard C, Terme M, Flament C, Taieb J, et al. (2005) CD4+CD25+ regulatory T cells inhibit natural killer cell functions in a transforming growth factor-beta-dependent manner. J Exp Med 202: 1075–1085.
40. Giroux M, Yurchenko E, St-Pierre J, Piccirillo CA, Perreault C (2007) T regulatory cells control numbers of NK cells and CD8alpha+ immature dendritic cells in the lymph node paracortex. J Immunol 179: 4492–4502.
41. Terme M, Chaput N, Combadiere B, Ma A, Ohteki T, et al. (2008) Regulatory T cells control dendritic cell/NK cell cross-talk in lymph nodes at the steady state by inhibiting CD4+ self-reactive T cells. J Immunol 180: 4679–4686.
42. Mehrotra PT, Donnelly RP, Wong S, Kanegane H, Geremew A, et al. (1998) Production of IL-10 by human natural killer cells stimulated with IL-2 and/or IL-12. J Immunol 160: 2637–2644.
43. Brady J, Hayakawa Y, Smyth MJ, Nutt SL (2004) IL-21 induces the functional maturation of murine NK cells. J Immunol 172: 2048–2058.
44. Maroof A, Beattie L, Zubairi S, Svensson M, Stager S, et al. (2008) Posttranscriptional regulation of Il10 gene expression allows natural killer cells to express immunoregulatory function. Immunity 29: 295–305.
45. Deniz G, Erten G, Kucuksezer UC, Kocacik D, Karagiannidis C, et al. (2008) Regulatory NK cells suppress antigen-specific T cell responses. J Immunol 180: 850–857.
46. Lee SH, Kim KS, Fodil-Cornu N, Vidal SM, Biron CA (2009) Activating receptors promote NK cell expansion for maintenance, IL-10 production, and CD8 T cell regulation during viral infection. J Exp Med 206: 2235–2251.
47. Perona-Wright G, Mohrs K, Szaba FM, Kummer LW, Madan R, et al. (2009) Systemic but not local infections elicit immunosuppressive IL-10 production by natural killer cells. Cell Host Microbe 6: 503–512.
48. Schulz U, Kreutz M, Multhoff G, Stoelcker B, Kohler M, et al. (2010) Interleukin-10 promotes NK cell killing of autologous macrophages by stimulating expression of NKG2D ligands. Scand J Immunol 72: 319–331.
49. Alter G, Kavanagh D, Rihn S, Luteijn R, Brooks D, et al. (2010) IL-10 induces aberrant deletion of dendritic cells by natural killer cells in the context of HIV infection. J Clin Invest 120: 1905–1913.
50. Shingu K, Kruschinski C, Luhrmann A, Grote K, Tschernig T, et al. (2003) Intratracheal macrophage-activating lipopeptide-2 reduces metastasis in the rat lung. Am J Respir Cell Mol Biol 28: 316–321.
51. Schmidt J, Welsch T, Jager D, Muhlradt PF, Buchler MW, et al. (2007) Intratumoural injection of the toll-like receptor-2/6 agonist 'macrophage-activating lipopeptide-2' in patients with pancreatic carcinoma: a phase I/II trial. Br J Cancer 97: 598–604.
52. Sutmuller RP, den Brok MH, Kramer M, Bennink EJ, Toonen LW, et al. (2006) Toll-like receptor 2 controls expansion and function of regulatory T cells. J Clin Invest 116: 485–494.
53. Liu H, Komai-Koma M, Xu D, Liew FY (2006) Toll-like receptor 2 signaling modulates the functions of CD4+ CD25+ regulatory T cells. Proc Natl Acad Sci U S A 103: 7048–7053.
54. Aramaki O, Inoue F, Takayama T, Shimazu M, Kitajima M, et al. (2005) Interleukin-10 but not transforming growth factor-beta is essential for generation and suppressor function of regulatory cells induced by intratracheal delivery of alloantigen. Transplantation 79: 568–576.
55. Yamazaki S, Dudziak D, Heidkamp GF, Fiorese C, Bonito AJ, et al. (2008) CD8+ CD205+ splenic dendritic cells are specialized to induce Foxp3+ regulatory T cells. J Immunol 181: 6923–6933.

OPEN ACCESS Freely available online

PLoS one

Development of Mouse Hepatocyte Lines Permissive for Hepatitis C Virus (HCV)

Hussein Hassan Aly[1], Hiroyuki Oshiumi[1], Hiroaki Shime[1], Misako Matsumoto[1], Taka Wakita[2], Kunitada Shimotohno[3], Tsukasa Seya[1]*

1 Department of Microbiology and Immunology, Hokkaido University Graduate School of Medicine, Sapporo, Hokkaido, Japan, 2 Department of Virology II, National Institute of Infectious Diseases, Shinjuku, Tokyo, Japan, 3 Research Institute, Chiba Institute of Technology, Narashino, Chiba, Japan

Abstract

The lack of a suitable small animal model for the analysis of hepatitis C virus (HCV) infection has hampered elucidation of the HCV life cycle and the development of both protective and therapeutic strategies against HCV infection. Human and mouse harbor a comparable system for antiviral type I interferon (IFN) induction and amplification, which regulates viral infection and replication. Using hepatocytes from knockout (ko) mice, we determined the critical step of the IFN-inducing/amplification pathways regulating HCV replication in mouse. The results infer that interferon-beta promoter stimulator (IPS-1) or interferon A receptor (IFNAR) were a crucial barrier to HCV replication in mouse hepatocytes. Although both IFNARko and IPS-1ko hepatocytes showed a reduced induction of type I interferons in response to viral infection, only IPS-1-/- cells circumvented cell death from HCV cytopathic effect and significantly improved J6JFH1 replication, suggesting IPS-1 to be a key player regulating HCV replication in mouse hepatocytes. We then established mouse hepatocyte lines lacking IPS-1 or IFNAR through immortalization with SV40T antigen. Expression of human (h)CD81 on these hepatocyte lines rendered both lines HCVcc-permissive. We also found that the chimeric J6JFH1 construct, having the structure region from J6 isolate enhanced HCV replication in mouse hepatocytes rather than the full length original JFH1 construct, a new finding that suggests the possible role of the HCV structural region in HCV replication. This is the first report on the entry and replication of HCV infectious particles in mouse hepatocytes. These mouse hepatocyte lines will facilitate establishing a mouse HCV infection model with multifarious applications.

Citation: Aly HH, Oshiumi H, Shime H, Matsumoto M, Wakita T, et al. (2011) Development of Mouse Hepatocyte Lines Permissive for Hepatitis C Virus (HCV). PLoS ONE 6(6): e21284. doi:10.1371/journal.pone.0021284

Editor: Jacques Zimmer, Centre de Recherche Public de la Santé (CRP-Santé), Luxembourg

Received May 13, 2011; **Accepted** May 24, 2011; **Published** June 22, 2011

Funding: This work was supported in part by Grants-in-Aid from the Ministry of Education, Science, and Culture (Specified Project for Advanced Research), the Ministry of Health, Labor, and Welfare of Japan, and the Hokkaido University Leader Development System in the Basic Interdisciplinary Research Areas (L station). Supports from Mitsubishi Foundation, Mochida Foundation, NorthTec Foundation Waxman Foundation and Yakult Foundation are gratefully acknowledged. The funders had no role in study design, data collection and analysis, decision to publish, or preparation of the manuscript.

Competing Interests: The authors have declared that no competing interests exist.

* E-mail: seya-tu@pop.med.hokudai.ac.jp

Introduction

Chronic hepatitis C virus (HCV) infection is a major cause of mortality and morbidity throughout the world infecting around 3.1% of the world's population [1]. The development of much needed specific antiviral therapies and an effective vaccine has been hampered by the lack of a suitable small animal model. The determinants restricting HCV tropism to human and chimpanzee hosts are unknown. Replication of HCV strain JFH1 has been demonstrated in mouse cells only upon antibody selection [2], highlighting the very limited replication efficiency. Human CD81 and occludin have been implicated as important entry receptors for retrovirus particles bearing HCV glycoproteins, HCV pseudoparticles (HCVpp), into NIH3T3 murine cells [3]. However, HCV infection, spontaneous replication and particle production by mouse cells have not yet been reported.

In mammalian cells, the host detects and responds to infection by RNA-viruses, including HCV, by primarily recognizing viral RNA through several distinct pathogen recognition receptors (PRRs), including the cell surface and endosomal RNA sensors Toll-like receptors 3 and 7 (TLR3 and TLR7), and the cytoplasmic RNA sensors retinoic acid-inducible gene I (RIG-I) and melanoma differentiation associated gene 5 (MDA5) [4]. The detection of virus infection by these receptors leads to the induction of interferons (IFNs) and their downstream IFN-inducible anti-viral genes through distinct signaling pathways [5]. Type I IFN is an important regulator of viral infections in the innate immune system [6]. Another type of IFN, IFN-lambda, affects the prognosis of HCV infection, and its response to antiviral therapy [7,8].

Mutations impairing the function of the RIG-I gene and the induction of IFN were essential in establishing HCV infectivity in human HuH7.5 cells [9]. Similarly, the HCV-NS3/4a protease is known to cleave IPS-1 adaptor molecule, inducing further downstream blocking of the IFN-inducing signaling pathway [10]. These data clearly demonstrate that the host RIG-I pathway is crucial for suppressing HCV proliferation in human hepatocytes. Using a similar strategy, we investigated whether suppressing the antiviral host innate immune system conferred any advantage on HCV proliferation in mouse hepatocytes. We examined the possibility of HCV replication in mice lacking the expression of key factors that modulate the type I IFN-inducing pathways. Only gene silencing of the IFN receptor (IFNAR) or IPS-1 was sufficient to establish spontaneous HCV replication in

mouse hepatocytes. To establish a cell line permissive for HCV replication, which is required for further *in vitro* studies of the HCV life cycle in mouse hepatocytes, we immortalized IFNAR- and IPS-1-knockout (ko) mice hepatocytes with SV40 T antigen. Upon expression of the human (h)CD81 gene, these newly established cell lines were able to support HCV infection for the first time in mouse hepatocytes. Viral factors required for HCV replication in mouse hepatocytes were also analyzed.

Results

IPS-1-mediated IFN signaling is important for HCV replication in mouse hepatocytes

As a first step in establishing HCV infection in mice, we tested the susceptibility of mouse hepatocytes to persistent expression of HCV proteins after RNA transfection. *In vitro* transcribed chimeric J6JFH1 RNA, in which the HCV structural and non-structural regions were from J6 and JFH1 isolates respectively, was transfected into hepatocytes from wild-type mice. We used a highly sensitive polyclonal antibody derived from HCV-patient serum for the detection of HCV proteins. No HCV proteins were detected five days after transfection (Fig. 1 A), suggesting that wild-type mouse hepatocytes were unable to maintain HCV replication. We then tried to find and block the pathway used by mouse hepatocytes for the detection of viral-RNA and the induction of IFN response. Mouse hepatocytes did not show the expression of either TLR3 or TLR7 as detected by RT-PCR, unlike IPS-1 and RIG-I which was fairly detected (Fig. S1), suggesting that the cytoplasmic RIG-I/IPS-1 pathway is the main pathway utilized by mouse hepatocytes for the detection of RNA viruses. We then checked the susceptibility of hepatocytes from TICAM-1ko, IPS-1ko and IFNARko mice to the prolonged expression of HCV proteins (Fig. 1B–D). Only IPS-1- and IFNARko mouse hepatocytes showed expression of J6JFH1 proteins five days after transfection (Fig. 1), indicating the importance of impaired IPS-1 and/or IFNAR receptors for HCV persistence. Similarly, the detection of the J6JFH1-RNA in transfected hepatocyte lines from various knockout mice showed higher levels in IPS-1 or IFNAR knockout cells compared to TICAM-1knockout cells in which a rapid decline of J6JFH1-RNA levels was noticed similar to the non-replicating control JFH1GND construct (Fig. S2). These data clearly suggest that the RIG-I/IPS-1 but not TLR3/TICAM-1 is the main pathway utilized for the detection of HCV-RNA and the induction of anti-viral immune response in mouse hepatocytes. Its suppression significantly improves HCV replication in mouse hepatocytes.

Establishment and characterization of immortalized mouse hepatocyte cell lines lacking expression of the IFNAR or IPS-1 gene

We further established mouse hepatocyte lines with disrupted IFNAR or IPS-1 genes through immortalization with SV40T antigen, and used these cell lines to study factors required for the HCV life cycle. Hepatocytes were transduced with SV40T-expressing lentivirus vectors. Six weeks after transduction, hepatocytes transduced with SV40T showed continuous proliferation and clonally proliferating hepatocyte lines were selected. SV40T-immortalized IFNARko and IPS-1ko clones were designated IRK (Fig. 2 A) and IPK (Fig. 2 B), respectively. 20 IRK and 19 IPK clones were picked up, of which IRK clones 2 and 4 (IRK2 and IRK4) and IPK clones 10 and 17 (IPK10 and IPK17) were most closely related to primary mouse hepatocytes in term of differentiation (Fig. 2 C) and were used in the following experiments. Expression of SV40T was confirmed by RT-PCR analysis (data not shown). IRK2, IRK4, IPK10 and IPK17, but not the non-hepatocytic NIH3T3 cells, displayed albumin and hepatocyte nuclear factor 4 (HNF4) expression similar to that observed in liver tissue, but did not express the bile duct marker, cytokeratin. IRK and IPK cells did not show expression of IFNAR and IPS-1 respectively (Fig. 2 C).

Replication of the HCV genome in IRK and IPK cells

To assess the permissiveness of the established cell lines to HCV replication, we transduced IRK4 and IPK17 cells with J6JFH1 RNA and monitored the HCV protein and RNA levels by IF (Fig. 3 A) and real time RT-PCR (Fig. 3 B). The number of cells expressing HCV proteins, as detected by IF, increased over time, indicating the continuous proliferation of J6JFH1 in these cells. However, the ratio between infected and non-infected cells did not significantly change over time for 7 days after transfection. Similarly, the amount of total J6JFH1 RNA in 1 μg of total cellular RNA was reasonably constant. By contrast, the level of

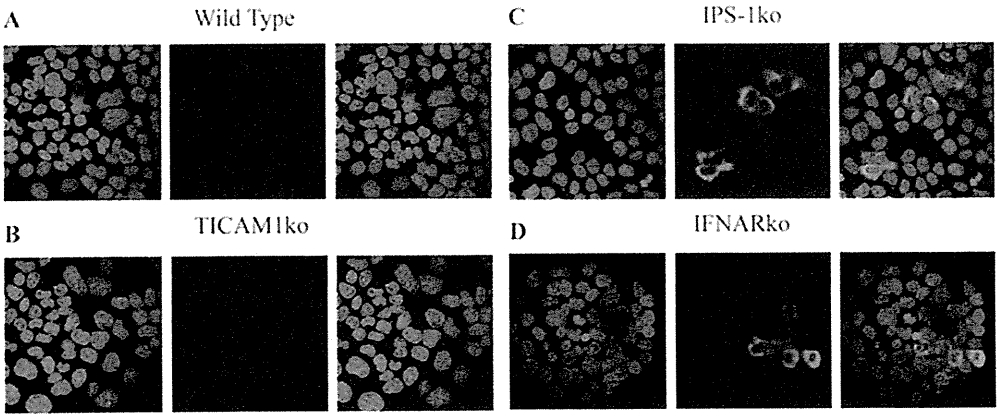

Figure 1. IF detection of of J6JFH1 proteins' expression 5 days after transfection of J6JFH1-RNA through electroporation into wild type (A), TICAM-1ko (B), IPS-1ko (C), and IFNARko (D), freshly isolated primary hepatocytes. A highly sensitive polyclonal antibody extracted from HCV-patient serum (AbS3) was used for the detection. Staining of the uninfected hepatocytes from different Ko mice was also performed and they showed negative for HCV proteins (data not shown).
doi:10.1371/journal.pone.0021284.g001

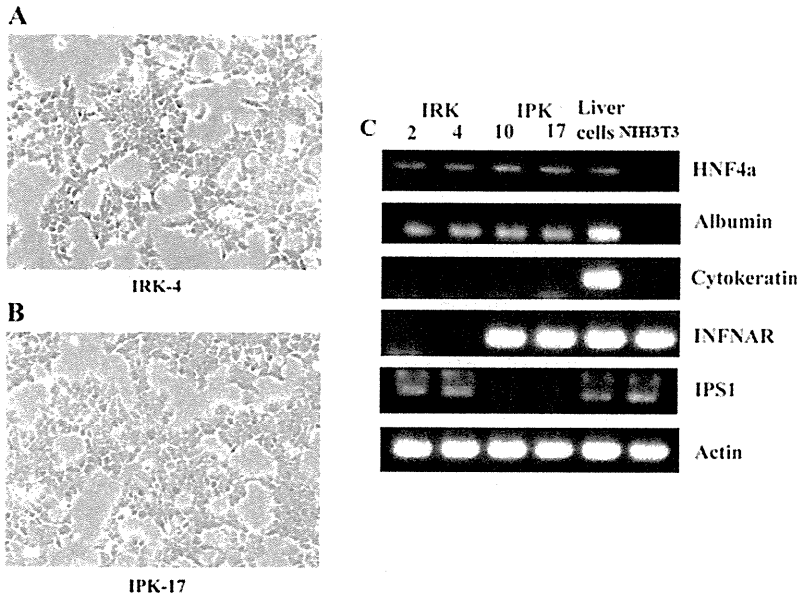

Figure 2. Morphological characteristics of IRK-4 (A) and IPK-17 (B) cells. (C) RT analysis for the expression of albumin, HNF4, cytokeratin, interferon A receptor, and IPS-1 in 2 IFNAR-KO cell lines (IRK2 and 4), 2 IPS-1-KO cell lines (IPK-10 and 17), total liver, and NIH3T3 cells.
doi:10.1371/journal.pone.0021284.g002

JFH1GND RNA carrying a mutation in NS5B hampering HCV replication, rapidly declined, indicating the requirement of continuous HCV replication for the maintenance of HCV positivity in the transfected mouse hepatocytes. Similar data were obtained from IRK2 and IPK10 cells (data not shown).

IPS-1-dependent/Interferon-independent pathway is responsible for HCV's cytopathic effect

In comparison to IPS-1ko hepatocytes, J6JFH1-RNA in IFNARko were lower and decreased further after its transfection, while higher stable levels of J6JFH1-RNA were maintained in IPS-1ko cells (Fig. 3 B and Fig. S2). Similarly, larger numbers of HCV-positive cells were detected in IPS-1ko hepatocytes compared with their IFNARko counterparts (Fig. 3 A), suggesting that the IPS-1 disruption benefits HCV replication in a distinct manner from IFNAR disruption. To measure the interferon induction after RNA virus infection in those cells, we used a highly infectious RNA-Virus (VSV) and measured the induction of interferon after its infection. All the interferons measured showed similar suppression of induction in IFNARko and IPS-1ko hepatocytes (Fig. 4). Surprisingly, cellular cytopathic effect that was monitored after transfection of J6JFH1-RNA was markedly reduced in IPS-1ko but not in IFNARko hepatocytes after transfection (Fig. 5A). This suppression was accompanied by an increase of J6JFH1-RNA levels in IPS-1ko cells, suggesting that minimal cellular damage induced by HCV replication in IPS-1-/- cells led to the improvement of HCV proliferation in mouse hepatocytes (Fig. 5B).Reduction of HCV-induced cellular cytotoxicity (Fig.5C), and improvement of HCV replication (Fig.5D) in wild type, and IFNAR-KO cells were found when we cultured the cells with a pan-caspase inhibitor, zVAD-fmk, 2 days before and after HCV-RNA transfection. We reasoned that the IPS-1 pathway rather than the IFNAR pathway capacitates hepatocytes to induce HCV-derived apoptotic cell death and its disruption resulted in the circumvention of cell death.

Human CD81 is required for HCV infection of mouse hepatocytes

Similar to the primary mouse hepatocytes, immortalized mouse hepatocytes showed the expression of all the mouse counterparts of human HCV entry receptors (Fig. S3). Human CD81 and hOccludin, but not other human HCV receptors such as SR-B1 or claudin1, have previously been reported to be essential for HCVpp entry into NIH3T3 mouse cells [3]. We then expressed hCD81 and/or hOccludin in IRK2 and IRK4 cells using lentivirus vectors. Using a MOI of 10, 95% transfection efficiency was achieved (Fig. S4) with lentivirus vector. We next tested the effect of these proteins on HCV particle (HCVcc) infection. Human CD81 alone was found to be required for J6JFH1 infection into all IRK and IPK cells tested (Fig. S5 and Fig. 6 A, and B). For the first time in mouse hepatocytes, HCV proteins were detected in nearly 1% of the cells used for infection. These data demonstrated the importance of hCD81 in establishing HCVcc infection in mouse hepatocytes.

Viral factors affecting HCV replication in mouse hepatocytes

After successfully establishing J6JFH1 infection in mouse hepatocytes, we attempted to infect these cells with other strains of HCV. Human CD81-expressing IPK17 cells were infected with full-length JFH1FL, however, no infection was detected (data not shown). This might be due to a problem in infection and/or replication. We further examined the replication efficiency of JFH1FL, the subgenomic JFH1 replicon and the J6JFH1 chimera in two different mouse hepatocyte lines and the HuH7.5.1 cell line. The persistent expression of HCV proteins was detected seven days after RNA transfection. Although HCV proteins were detected in HuH7.5.1 cells in all cases (Fig. 7 C), only J6JFH1 proteins were detected in the mouse hepatocyte lines, suggesting for the first time the importance of the J6 structural region for the replication of HCV in mouse hepatocytes (Fig. 7 A, and B).

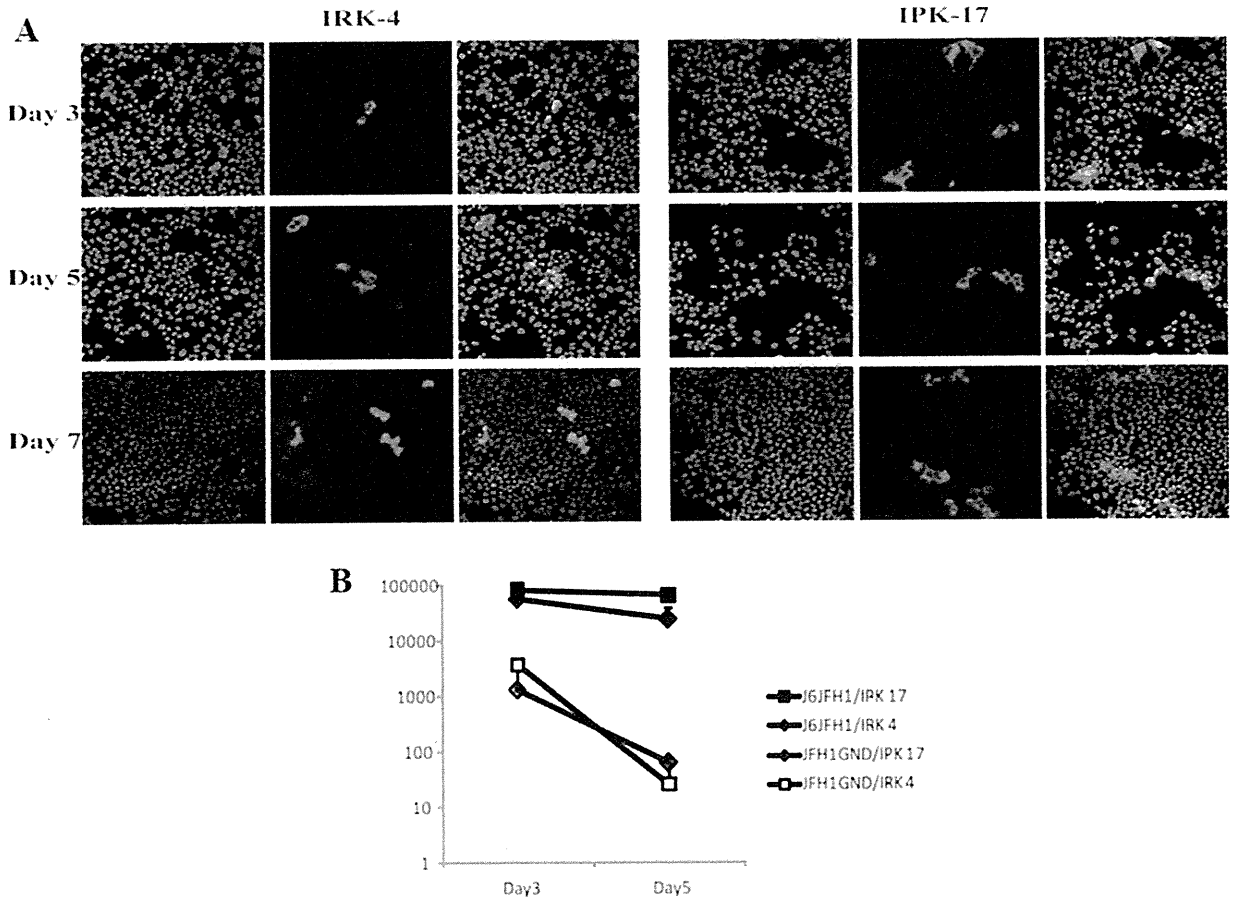

Figure 3. Proliferation of HCV in IRK4 and IPK17 cells over time as detected by immunofluorescence staining of NS5a protein using the CL1 rabbit polyclonal antibody (A) and by quantitative real-time RT-PCR analysis of HCV-RNA levels (B). JFH1GND was used as a negative control to exclude non replicating HCV-RNA. The data plotted represent the average +/− STD of 3 different experiments.
doi:10.1371/journal.pone.0021284.g003

Discussion

Gene silencing of either IPS-1 or IFNAR significantly improves HCV replication and persistence in mouse hepatocytes compared with wild-type or TICAM-1ko mice. This result demonstrated the importance of the IPS-1 pathway rather than the TICAM-1 pathway in the induction of type I IFN by HCV infection, and revealed that the IFNAR amplification pathway confers resistance to HCV in mouse hepatocytes independently of TICAM-1. In accordance with our data, HCV-NS3/4A protease is known to cleave the IPS-1 and/or RIG-I-complement molecules including DDX3 and Riplet in humans to overcome the host innate immune response, showing the importance of RIG-I/IPS-1 pathway suppression in the establishment of HCV infection [10,11,12].

To further study factors affecting the HCV life cycle in mouse hepatocytes, we established IPK and IRK immortalized mouse hepatocyte lines by transduction with SV40T antigen. The established hepatocytes cell lines showed expression of HNF4, a major hepatocyte transcription factor, required for hepatocyte differentiation and liver-specific gene expression [13]. The maintenance of hepatocellular functions was demonstrated by continuous expression of hepatocyte specific differentiation marker, albumin, and the lack of expression of the bile duct marker, cytokeratin. The close resemblance of these cell lines to primary mouse hepatocytes is crucial to ensure the physiological relevance of factors identified in these cell lines that affect the HCV life cycle.

It is worth noting that HCV replication in IPS-1ko was higher than that in IFNARko hepatocytes. Since IPS-1 is present upstream of IFNAR in the IFN-amplification pathway, this higher J6JFH1 replication efficiency in IPS-1ko hepatocytes suggested the presence of an additive factor affecting HCV replication other than the induction of IFNAR-mediated type I IFN. This enhanced replication efficiency was also not accompanied by the induction of other interferon types, but was correlated with the reduction of HCV-induced apoptosis in mouse hepatocytes. This data clearly demonstrates that IPS-1 is playing an important role in the regulation of HCV infection in mouse hepatocytes through two different pathways, the IFN-induction pathways and another new IFN-independent pathway, leading to apoptotic cell death and elimination of HCV-harboring hepatocytes. The cytopathic effect of HCV infection in human cells is still contradictory. Although, some reports showed the induction of apoptosis and cell death by HCV infection in human hepatocytes [14,15,16], others showed suppression of apoptosis by HCV proteins [17,18]. This difference may be due to the different cell lines used in the different studies. Almost all the studies reporting HCV-induced apoptosis used

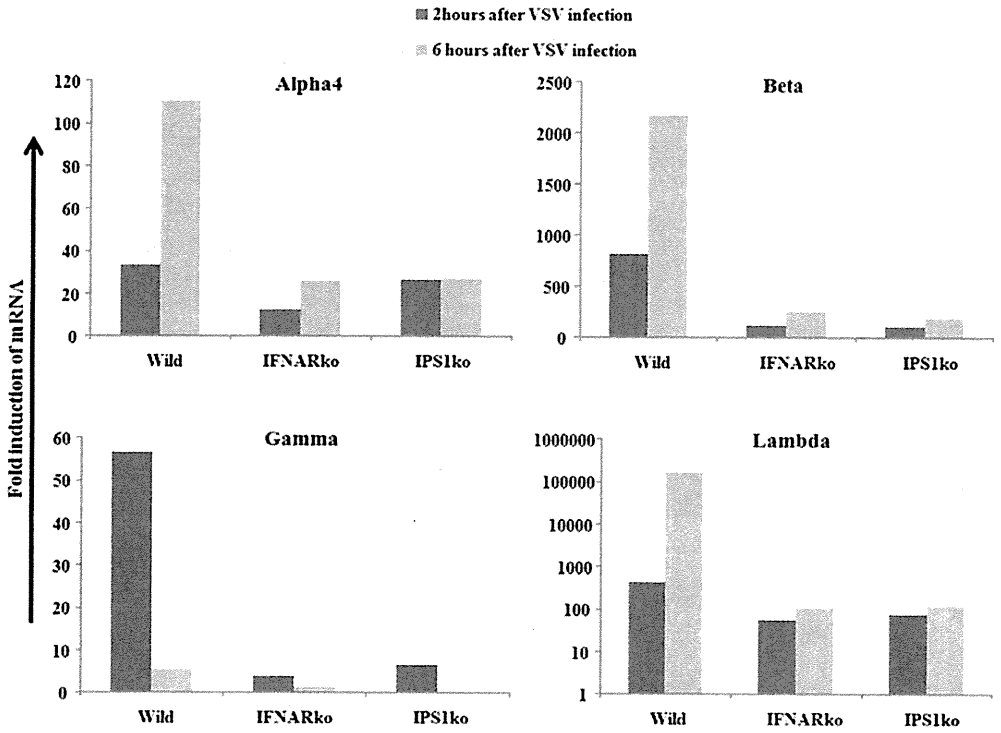

Figure 4. Wild type, IFNARko, and IPS-1ko mice hepatocytes were infected with mock or VSV virus, 2 and 6 hours later, total RNA was extracted from the cells, and interferon alpha, beta, gamma and lambda mRNA induction levels were measured by real-time RT-PCR. Similar results were obtained from 2 different experiments, each was performed in duplicates. The data plotted represent the mean duplicate readings in one of them.
doi:10.1371/journal.pone.0021284.g004

hepatocellular carcinoma cell lines. Since it has been established that the inability to undergo apoptosis is essential for the development of cancer [19,20,21], our use of immortalized, non-cancerous hepatocytes may make it possible to reproduce the physiological response of the cells to HCV infection more closely. The IPS-1 regulation of cell death following the introduction of HCV-RNA may also regulate the effector cell function. It is likely that hepatocyte debris generated secondary to intrinsic production of viral dsRNA in HCV-infected hepatocytes affect the antiviral effector response of the immune system through maturation of dendritic cells [22]. Hence, the effector cell activation may be enhanced by the induction of cell death through the IPS-1 pathway in hepatocytes which may facilitate producing dsRNA-containing debris.

In comparison to the JFH1GND construct with deficient replication that showed a rapid reduction in its RNA levels over time after transfection into mouse hepatocytes, J6JFH1 RNA was detected at four-log higher levels and was maintained at a relatively stable levels in IPS-1ko hepatocytes. Although the number of mouse cells expressing HCV proteins was found to increase over time, as detected by IF, the ratio between HCV-negative and -positive cells did not show any significant change for 7 days after transfection and increased after 10 days (data not shown). This indicates a negative selection of HCV-bearing cells over time which may be due to slower cellular replication, or loss of HCV replication. Another possibility may be that HCV infection is affected by the presence of an inhibitory factor possibly triggered by HCV replication or the lack of a human host factor required for HCV replication. Due to the initial replication of HCV in the transfected IPK and IRK mouse hepatocytes for the first 7 days and the establishment of infection, we favor the presence of a possible inhibitory factor that may be triggered by HCV replication. Another factor that also limits HCV spread in mouse hepatocytes is the failure of HCV to produce infectious particles in these cells (data no shown).

Using this newly established immortalized mouse hepatocyte line, we found that although J6JFH1, JFH1FL and the subgenomic JFH1 replicon all share a similar non-structural region derived from isolate JFH1 that is required for HCV replication, and although all of these constructs can replicate efficiently in HuH7.5.1 cells, strikingly, only J6JFH1 carrying the J6 structural region replicated in mouse hepatocytes. This indicates the importance of the J6 structural region and/or the chimeric construct between J6 and JFH1 for HCV replication in mouse hepatocytes. Structural regions are known to be important for HCV entry and/or particle formation [23], but this is the first time that their importance in replication in HCV-bearing cells has been demonstrated. This finding clearly shows the importance of non-hepatoma cell lines with less genetic abnormalities and mutations for the discovery of new aspects of the life cycle of HCV.

Although, the co-expression of human CD81 and Occludin genes was found to be important for HCVpp entry into murine NIH3T3 cells [3], the expression of hCD81 alone was sufficient for J6JFH1 entry into mouse hepatocytes. This may be explained by the different cell lines used in the different studies. In contrast to NIH3T3 cells, we used immortalized hepatocytes that showed close physiological resemblance to primary mouse hepatocytes and showed the expression of all the mouse counterparts of HCV entry

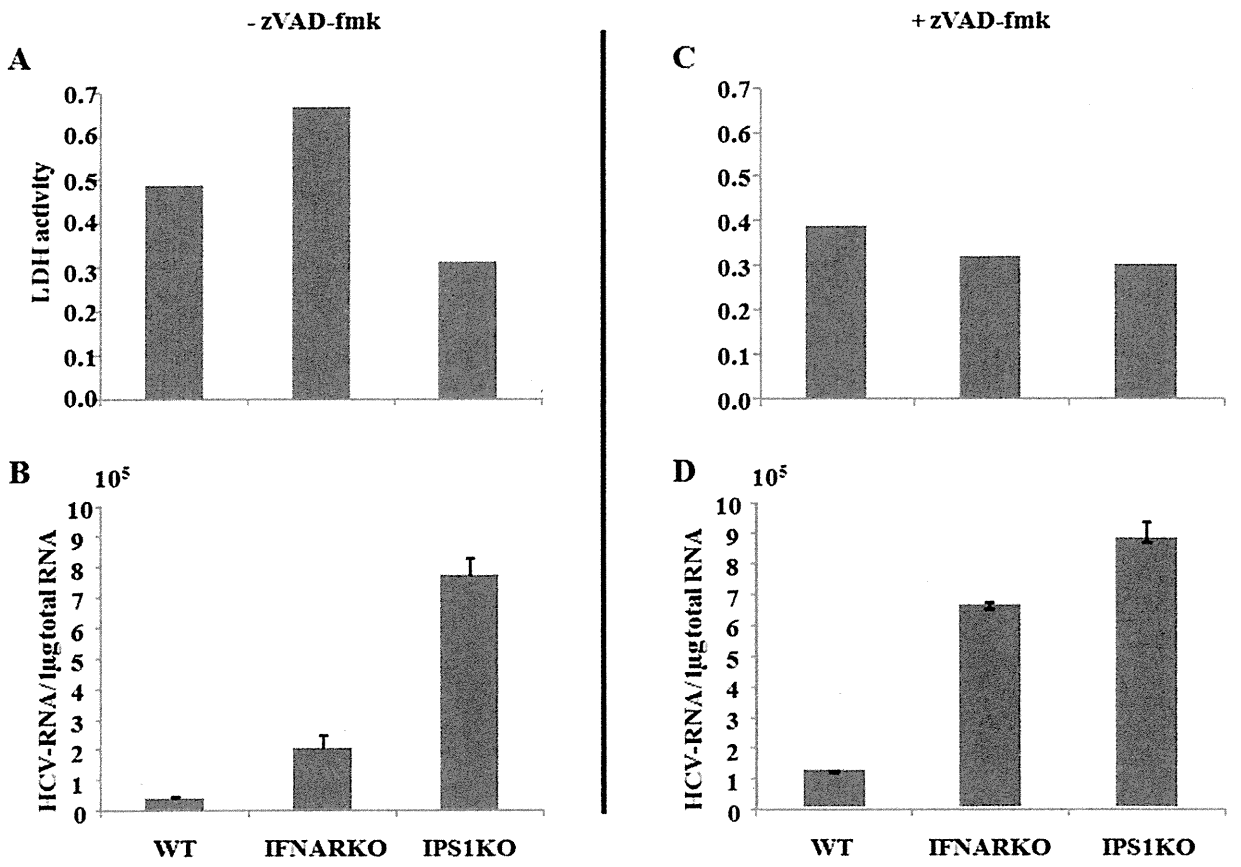

Figure 5. Measurement of J6JFH1 mediated cytopathic effect in wild type, IFNARko, and IPS-1ko mouse hepatocytes. Cultrure medium were left untreated (A;B) or treated with 20 μM of zVAD-fmK (C;D) 2 days before and after J6JFH1-RNA transfection. One day after transfection of J6JFH1-RNA, culture medium was discarded and cells were washed with PBS. A new medium was added and cells were cultured for another 24 hours. The LDH activity in the culture medium was measured in 2 different experiments in duplicates and showed similar results, the average levels of a duplicate from a single experiment was plotted (A, C). HCV-RNA titers in the cells were also measured using real-time RT-PCR (B, D), the data shown represent the mean +/− STD of 3 different experiments.
doi:10.1371/journal.pone.0021284.g005

receptors. A study from a different group showed that adaptive mutations in HCV envelope proteins allowing its interaction with murine CD81 is enough for efficient HCVpp entry without the expression of any human entry receptors in murine cells [24]. This report, together with ours, suggest that CD81 is the main human host restriction factor for HCV entry, and that overcoming this problem either by HCV adaptation to murine CD81, or the expression of human CD81 in murine hepatocytes is essential for HCV entry. Although our lentivirus transfection efficiency with CD81 was around 95% in IPK and IRK clones, only 1% of the cells were prone to infection with HCVcc. Also, HCVpp showed lower entry levels in those cells compared to HuH7.5.1 cells (Fig. S6). This suggests that hCD81 expression is the minimum and most crucial requirement for HCV entry into mouse hepatocytes. The discovery and expression of other co-receptors facilitating HCV entry in human cells is still required for efficient and robust HCV infection.

In summary, the suppression of IPS-1 is important for the establishment of HCV infection and replication in mouse hepatocytes through the suppression of both interferon induction and interferon independent J6JFH1-induced cytopathic effect. We have established hepatocytes lines from IPS-1 and IFNARko mice that support HCV replication and infection. These cell lines will be very useful in identifying other species restriction factors and viral determinants required for further establishment of a robust and efficient HCV life cycle in mouse hepatocytes. Using those cells, we showed for the first time the importance of HCV structural region for viral replication. IRF3ko mouse embryo fibroblasts (MEFs) were previously shown to support HCV replication more efficiently than wild MEFs [25]. Since the knockout of IPS-1 mainly suppresses signaling in response to virus RNA detection, and maintains an intact IFN response to other stimulants, it may result in minimum interference to adaptive immune responses as compared to IRF3 or IFNARko. Therefore, further development of hCD81-transgenic IPS-1ko mice may serve as a good model for the study of immunological responses against HCV infection. This mouse model can be used as a backbone for any further future models supporting robust HCV infectivity for the study of HCV pathogenesis, propagation and vaccine development.

Material and Methods

Cell culture

HuH7.5.1 cells were cultured in high-glucose Dulbecco's modified Eagle's medium (DMEM; Gibco/Invitrogen, Tokyo, Japan) supplemented with 2 mM L-glutamine, 100 U of penicillin/ml, 100 μg of

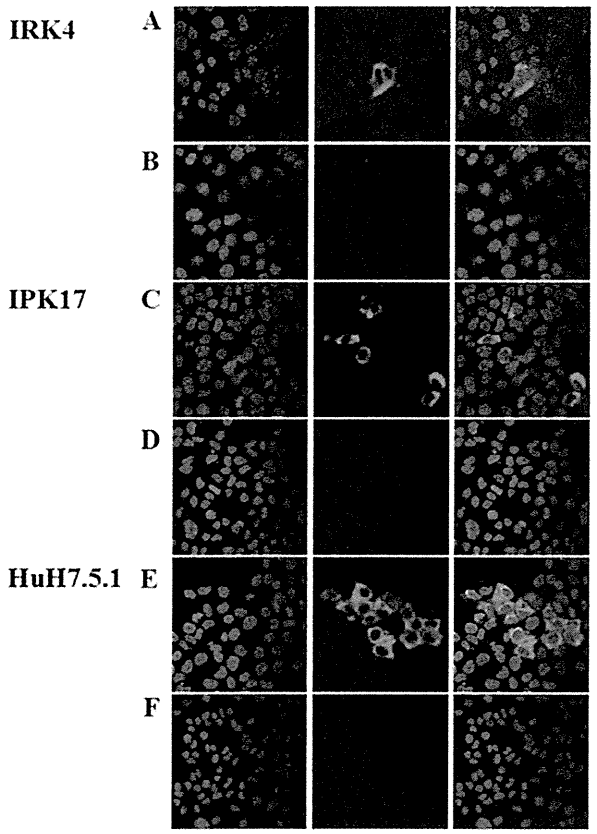

Figure 6. J6JFH1 infection into IRK-4 and IPK17 cells. HCV-NS5A protein detection in mouse IRK4 (A,B) and IPK17 (C,D) and human 7.5.1 cells (E,F). The cells were transduced with lentivirus expressing human CD81 gene at 10 MOI. 48 hours later the cells were infected with 100 times concentrated supernatant medium, collected during 1 week after transfection of HuH7.5.1 cells with J6JFH1-RNA (A, C, and E) or JFH1GND-RNA (B, D, and F).
doi:10.1371/journal.pone.0021284.g006

streptomycin/ml and 10% fetal bovine serum. Mouse primary hepatocytes were isolated from the liver using collagenase perfusion through the inferior vena cava (IVC), while clamping the animal's intrathoracic extension. Hepatocyte isolation and perfusion control were performed as previously described [26]. Primary and immortalized hepatocytes were cultured in a similar medium supplemented with: HEPES (Gibco/Invitrogen), 20 mmol/L; L-proline, 30 μg/mL; insulin (Sigma, St. Louis, MO, USA), 0.5 μg/mL; dexamethasone (Wako, Osaka, Japan), 1×10^{-7} mol/L; $NaHCO_3$, 44 mmol/L; nicotinamide (Wako), 10 mmol/L; EGF (Wako), 10 ng/mL; L-ascorbic acid 2-phosphate (Wako), 0.2 mmol/L; and MEM-non essential amino acids (Gibco/Invitrogen), 1%.

Gene-disrupted mice

All mice were backcrossed with C57BL/6 mice more than seven times before use. Toll-like receptor adaptor molecule 1 (TICAM-1) ko [27] and IPS-1ko mice [28] were generated in our laboratory (detailed information regarding the IPS-1 mice will be presented elsewhere). All mice were maintained under specific-pathogen-free conditions in the animal facility of the Hokkaido University Graduate School of Medicine (Japan).

RNA extraction, reverse transcriptase polymerase chain reaction (RT-PCR) and real-time RT-PCR

RNA was extracted from cultured cells using Trizol reagent (Invitrogen, San Diego, CA, USA) according to the manufacturer's protocol. Using 1 μg of total RNA as a template, we performed RT-PCR and real-time RT-PCR as previously described [29,30].

In vitro RNA transcription, transfection and preparation of J6JFH1 and Jfh1 viruses

In vitro RNA transcription, transfection into HuH7.5.1 or mouse hepatocytes, and preparation of J6JFH1 and JFH1 viruses, were all performed as previously reported [31]. RNA transfection into human and mouse hepatocytes was performed by electroporation using a Gene Pulser II (Bio-Rad, Berkeley, California) at 260 V and 950 Cap.

HCV infection

J6JFH1 and JFH1 concentrated medium were adjusted to contain a similar RNA copy number by real-time RT-PCR. 2×10^4 cells/well were cultured in 8-well glass chamber slides. After 24 hours, the medium was removed and replaced by concentrated medium containing JFH1 or J6JFH1 viruses. After three hours, the concentrated medium was removed, cells were washed with PBS and incubated in fresh medium for 48 hours, before the detection of infection.

Lentivirus construction, titration and infection

The gene encoding T antigen from simian virus was cloned from plasmid CSII-EF-SVT [32]. The genes encoding human CD81 and occludin were cloned from HuH-7.5.1 cells using the Zero Blunt TOPO PCR Cloning Kit (Invitrogen) according to the manufacturer's protocol. These genes were then inserted into the GFP reporter gene-containing lentiviral expression (pLBIG) vector using the *Eco*RI and *Xho*I restriction sites for SV40T and hCD81, and the *Xba*I and *Xho*I restriction sites for hOccludin. Lentivirus expression vectors were then constructed as previously described [27]. GFP expression was used for the titration of lentivirus vectors, and a multiplicity of infection (MOI) of 10 was used for the infection of mouse cells. Forty-eight hours after the transfection of hCD81 and/or hOccludin, cells were trypsinized and counted. Then, 2×10^4 cells/well were cultured in 8-well glass chamber slides for HCV infection and 5×10^4 cells/well were cultured in 12-well plates, along with 1 ml of medium containing HCVpp, for HCV entry experiments.

HCVpp construction and the detection of luciferase expression

HCVpp containing the E1 and E2 proteins from HCV isolate J6 and expressing the luciferase reporter gene were a kind gift from Dr. Thomas Pietschmann at the TWINCORE Center for Experimental and Clinical Infection Research, Germany. The production of HCVpp and the measurement of luciferase levels were performed as previously described [33].

Indirect immunofluorescence (IF)

IF expression of HCV proteins was detected in the infected cells using antibodies in the serum of chronic HCV patients or rabbit IgG anti-NS5A antibody (Cl-1) (both kind gifts from K. Shimotohno, Chiba Institute of Technology, Japan). Goat anti-human IgG Alexa 594 and goat anti-rabbit Alexa 594 (Invitrogen) were used as secondary antibodies, respectively. Fluorescence

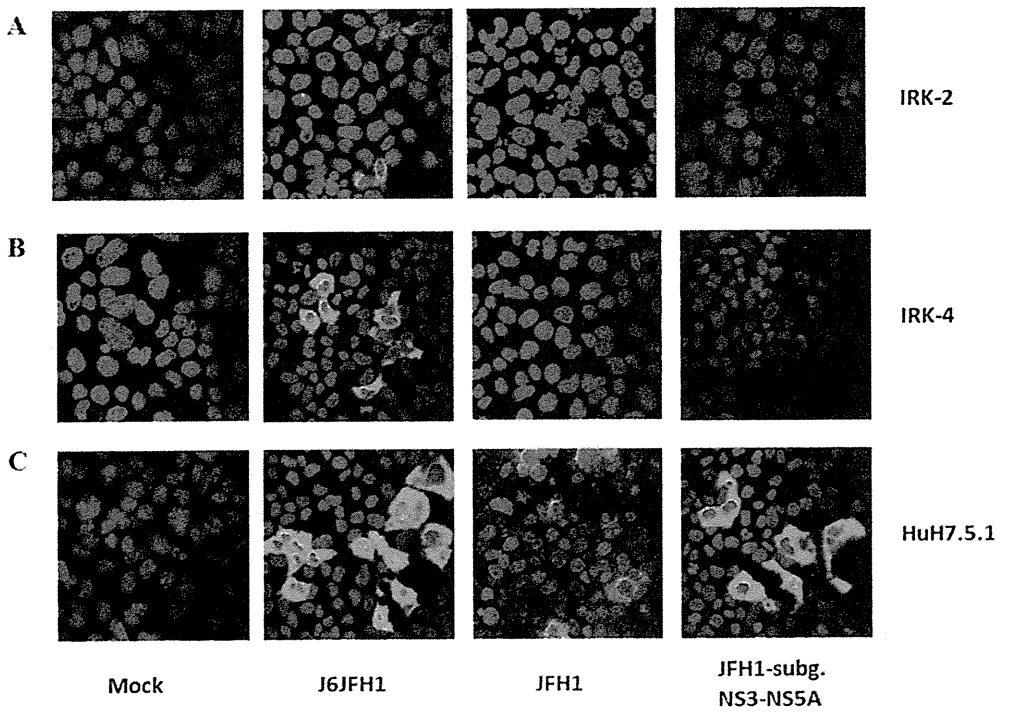

Figure 7. Detection of HCV-NS5A protein in IRK-2 (A), IRK-4 (B) and HuH-7.5 cells (C) by IF 5 days after transfection with J6JFH1, FL-JFH1 or subgenomic JFH1-RNA.
doi:10.1371/journal.pone.0021284.g007

detection was performed on a ZEISS LSM 510 Meta confocal microscope (Zeiss, Jena, Germany).

Detection of cell death

Culture medium was collected from HCV infected and control cells and used for measuring lactate dehydrogenase (LDH) levels using an LDH cytotoxicity detection kit (Takara Biomedicals, Tokyo, Japan). Light absorbance was then measured according to the manufacturer's protocol.

Ethic Statement

This study was carried out in strict accordance with the recommendations in the Guide for the Care and Use of Laboratory Animals of the National Institutes of Health. The protocol was approved by the Committee on the Ethics of Animal Experiments in the Animal Safety Center, Hokkaido University, Japan. All mice were used according to the guidelines of the institutional animal care and use committee of Hokkaido University, who approved this study as ID number: 08-0243, " Analysis of immune modulation by toll-like receptors".

Supporting Information

Figure S1 RT detection of TLR3, TLR7, RIG-I, and IPS-1 expression in mouse hepatocytes. GAPDH expression was used as internal control, and RNA from CD11c+ spleenocytes (dendritic cells) was used as positive control.
(TIF)

Figure S2 Proliferation of HCV in IPS-1, TICAM-1(TRIF) and IFNAR-knockout mouse hepatocytes over time as detected by quantitative real-time RT-PCR analysis of HCV-RNA levels. JFH1GND transfection into IPS-1 knockout cells was used as a negative control to exclude non replicating HCV RNA. The data plotted represent the average +/− STD of 3 different experiments.
(TIF)

Figure S3 RT detection of CD81, Occludin, Claudin 1, SRB1, and LDL receptor expression in primary, IRK4 and IPK17 mouse hepatocytes. GAPDH expression was used as internal control.
(TIF)

Figure S4 Estimation of the transfection efficiency of lentivirus vector expressing green fluorescent protein (GFP) as a reporter, together with hCD81 or hOccludin. 48 hours after transfection with the lentivirus vector, cells were trypsinized and GFP positive cells were detected by BD FACSCalibur (BD Biosciences).
(TIF)

Figure S5 HCV infection of IRK2 cells transfected with lentivirus expressing hCD81 and/or hOccludin. IRK2 cells were transfected with lentivirus expressing empty vector (A), hCD81 (B), hOccludin (C) or hCD81 and hOccludin (D) at a MOI of 10. After 48 hours, the cells were infected with concentrated J6JFH1 transfected 7.5.1 culture medium. After a further three hours, cells were washed with PBS and incubated in fresh medium. After another 48 hours, HCV infection was examined through the detection of HCV-NS5a protein expression by immunofluorescence staining.
(TIF)

Figure S6 HCVpp entry into mouse cells. A similar number of IPK17 and HuH7.5.1 were cultured in triplicate. IPK17 cells were only transfected with lentivirus expressing hCD81, while HuH7.5.1 cells were transfected with empty vector at a MOI of

10. After 48 hours, the medium was replaced with a new medium containing mock VSVG-pp or HCVpp expressing luciferase. After another 48 hours, pseudoparticles entry was determined by measuring the luciferase activity. In order to compare the HCVpp entry between IPK17 and HuH7.5.1 cells, the luciferase expression from VSV-Gpp entry was used an internal control, while that from HCVpp was plotted relatively.
(TIF)

Acknowledgments

We want to thank Dr. Michinori Kohara (Tokyo Metropolitan Institute for Medical Science, Tokyo, Japan); Dr. Tadatsugu Taniguchi (University of Tokyo, Yokyo, Japan); Dr. Thomas Pietschmann (Division of Experimental Virology, TWINCORE, Hannover, Germany); and Dr. Makoto Hijikata (The Institute for Virus Research, Kyoto University, Japan) for their generous supply of research material. Dr. Hussein H. Aly was supported by a JSPS postdoctoral fellowship from the Japan Society for the Promotion of Science.

Author Contributions

Conceived and designed the experiments: HHA TS. Performed the experiments: HHA HO. Analyzed the data: HHA MM HO HS TS. Contributed reagents/materials/analysis tools: KS TW. Wrote the paper: HHA.

References

1. Seto WK, Lai CL, Fung J, Hung I, Yuen J, et al. (2010) Natural history of chronic hepatitis C: Genotype 1 versus genotype 6. J Hepatol.
2. Uprichard SL, Chung J, Chisari FV, Wakita T (2006) Replication of a hepatitis C virus replicon clone in mouse cells. Virol J 3: 89.
3. Ploss A, Evans MJ, Gaysinskaya VA, Panis M, You H, et al. (2009) Human occludin is a hepatitis C virus entry factor required for infection of mouse cells. Nature 457: 882–886.
4. Diamond MS (2009) Mechanisms of evasion of the type I interferon antiviral response by flaviviruses. J Interferon Cytokine Res 29: 521–530.
5. O'Neill LA, Bowie AG (2010) Sensing and signaling in antiviral innate immunity. Curr Biol 20: R328–333.
6. Platanias LC (2005) Mechanisms of type-I- and type-II-interferon-mediated signalling. Nat Rev Immunol 5: 375–386.
7. Tanaka Y, Nishida N, Sugiyama M, Kurosaki M, Matsuura K, et al. (2009) Genome-wide association of IL28B with response to pegylated interferon-alpha and ribavirin therapy for chronic hepatitis C. Nat Genet 41: 1105–1109.
8. Thompson AJ, Muir AJ, Sulkowski MS, Ge D, Fellay J, et al. (2010) Interleukin-28B polymorphism improves viral kinetics and is the strongest pretreatment predictor of sustained virologic response in genotype 1 hepatitis C virus. Gastroenterology 139: 120–129. e118.
9. Sumpter R, Jr., Loo YM, Foy E, Li K, Yoneyama M, et al. (2005) Regulating intracellular antiviral defense and permissiveness to hepatitis C virus RNA replication through a cellular RNA helicase, RIG-I. J Virol 79: 2689–2699.
10. Foy E, Li K, Sumpter R, Jr., Loo YM, Johnson CL, et al. (2005) Control of antiviral defenses through hepatitis C virus disruption of retinoic acid-inducible gene-I signaling. Proc Natl Acad Sci U S A 102: 2986–2991.
11. Oshiumi H, Ikeda M, Matsumoto M, Watanabe A, Takeuchi O, et al. (2010) Hepatitis C virus core protein abrogates the DDX3 function that enhances IPS-1-mediated IFN-beta induction. PLoS One 5: e14258.
12. Oshiumi H, Miyashita M, Inoue N, Okabe M, Matsumoto M, et al. (2010) The ubiquitin ligase Riplet is essential for RIG-I-dependent innate immune responses to RNA virus infection. Cell Host Microbe 8: 496–509.
13. Ishiyama T, Kano J, Minami Y, Iijima T, Morishita Y, et al. (2003) Expression of HNFs and C/EBP alpha is correlated with immunocytochemical differentiation of cell lines derived from human hepatocellular carcinomas, hepatoblastomas and immortalized hepatocytes. Cancer Sci 94: 757–763.
14. Berg CP, Schlosser SF, Neukirchen DK, Papadakis C, Gregor M, et al. (2009) Hepatitis C virus core protein induces apoptosis-like caspase independent cell death. Virol J 6: 213.
15. Deng L, Adachi T, Kitayama K, Bungyoku Y, Kitazawa S, et al. (2008) Hepatitis C virus infection induces apoptosis through a Bax-triggered, mitochondrion-mediated, caspase 3-dependent pathway. J Virol 82: 10375–10385.
16. Zhu H, Dong H, Eksioglu E, Hemming A, Cao M, et al. (2007) Hepatitis C virus triggers apoptosis of a newly developed hepatoma cell line through antiviral defense system. Gastroenterology 133: 1649–1659.
17. Ray RB, Meyer K, Ray R (1996) Suppression of apoptotic cell death by hepatitis C virus core protein. Virology 226: 176–182.
18. Mankouri J, Dallas ML, Hughes ME, Griffin SD, Macdonald A, et al. (2009) Suppression of a pro-apoptotic K+ channel as a mechanism for hepatitis C virus persistence. Proc Natl Acad Sci U S A 106: 15903–15908.
19. Ladu S, Calvisi DF, Conner EA, Farina M, Factor VM, et al. (2008) E2F1 inhibits c-Myc-driven apoptosis via PIK3CA/Akt/mTOR and COX-2 in a mouse model of human liver cancer. Gastroenterology 135: 1322–1332.
20. Lowe SW, Lin AW (2000) Apoptosis in cancer. Carcinogenesis 21: 485–495.
21. Schulze-Bergkamen H, Krammer PH (2004) Apoptosis in cancer--implications for therapy. Semin Oncol 31: 90–119.
22. Ebihara T, Shingai M, Matsumoto M, Wakita T, Seya T (2008) Hepatitis C virus-infected hepatocytes extrinsically modulate dendritic cell maturation to activate T cells and natural killer cells. Hepatology 48: 48–58.
23. Mateu G, Donis RO, Wakita T, Bukh J, Grakoui A (2008) Intragenotypic JFH1 based recombinant hepatitis C virus produces high levels of infectious particles but causes increased cell death. Virology 376: 397–407.
24. Bitzegeio J, Bankwitz D, Hueging K, Haid S, Brohm C, et al. (2010) Adaptation of hepatitis C virus to mouse CD81 permits infection of mouse cells in the absence of human entry factors. PLoS Pathog 6: e1000978.
25. Lin LT, Noyce RS, Pham TN, Wilson JA, Sisson GR, et al. (2010) Replication of subgenomic hepatitis C virus replicons in mouse fibroblasts is facilitated by deletion of interferon regulatory factor 3 and expression of liver-specific microRNA 122. J Virol 84: 9170–9180.
26. Ishigami A, Fujita T, Handa S, Shirasawa T, Koseki H, et al. (2002) Senescence marker protein-30 knockout mouse liver is highly susceptible to tumor necrosis factor-alpha- and Fas-mediated apoptosis. Am J Pathol 161: 1273–1281.
27. Akazawa T, Ebihara T, Okuno M, Okuda Y, Shingai M, et al. (2007) Antitumor NK activation induced by the Toll-like receptor 3-TICAM-1 (TRIF) pathway in myeloid dendritic cells. Proc Natl Acad Sci U S A 104: 252–257.
28. Ebihara T, Azuma M, Oshiumi H, Kasamatsu J, Iwabuchi K, et al. (2010) Identification of a polyI:C-inducible membrane protein that participates in dendritic cell-mediated natural killer cell activation. J Exp Med 207: 2675–2687.
29. Aly HH, Qi Y, Atsuzawa K, Usuda N, Takada Y, et al. (2009) Strain-dependent viral dynamics and virus-cell interactions in a novel in vitro system supporting the life cycle of blood-borne hepatitis C virus. Hepatology 50: 689–696.
30. Aly HH, Shimotohno K, Hijikata M (2009) 3D cultured immortalized human hepatocytes useful to develop drugs for blood-borne HCV. Biochem Biophys Res Commun 379: 330–334.
31. Wakita T, Pietschmann T, Kato T, Date T, Miyamoto M, et al. (2005) Production of infectious hepatitis C virus in tissue culture from a cloned viral genome. Nat Med 11: 791–796.
32. Aly HH, Watashi K, Hijikata M, Kaneko H, Takada Y, et al. (2007) Serum-derived hepatitis C virus infectivity in interferon regulatory factor-7-suppressed human primary hepatocytes. J Hepatol 46: 26–36.
33. Haid S, Windisch MP, Bartenschlager R, Pietschmann T (2010) Mouse-specific residues of claudin-1 limit hepatitis C virus genotype 2a infection in a human hepatocyte cell line. J Virol 84: 964–975.

Molecular Immunology 48 (2011) 1589–1590

Contents lists available at ScienceDirect

Molecular Immunology

journal homepage: www.elsevier.com/locate/molimm

Addendum

Addendum to "Strain-to-strain difference of V protein of measles virus affects MDA5-mediated IFN- -inducing potential" [Mol. Immunol. 48(4) (2011) 497–504]

Tsukasa Seya

Department of Microbiology and Immunology, Graduate School of Medicine, Hokkaido University, Kita-ku, Sapporo 060-8638, Japan

article info

Article history:
Received 9 April 2011
Accepted 9 April 2011
Available online 30 April 2011

abstract

Measles virus (MV) V protein blocks type I IFN signaling in MV-infected cells. Previous studies suggested that some MV strains could release the V protein-mediated type I IFN suppression in affected cells by two distinct modes: V protein mutation and production of DI RNA. These two modes of type I interferon regulation involves the IPS-1 (MAVS, Cardif, VISA) pathway (Takaki et al., 2011. Mol. Immunol. 48(4), 497–504). We add the comment to this previous issue that the release of the V protein-mediated suppression of type I IFN occurs only by a laboratory-adapted strain of Edmonston.

Dear Editor,

Recently, we received a comment that the C272R MV strain we used in our recent publication in Molecular Immunology (Takaki et al., 2011) is a recombinant Edmonston (ED) strain, thus not a representative ED vaccine strain. We searched the NCBI database (www.ncbi.nih.gov/nuccore/1041617) for Edmonston strain and found that this comment is right. The clone we used is very similar to that deposited in the bank as Measles virus (strain Edmonston B) RNA (infectious cDNA clone), GenBank: Z66517.1. The ED vaccine lineage was described in Parks et al. (2001). According to the sequence definition, this strain may be originated from the reported recombinant virus of an ED infectious strain. As we did not mention in the paper (Takaki et al., 2011) that this ED strain is originated from the vaccine or reverse-transcribed ED, we describe this addendum to indicate that the ED strain we used is a laboratory-adapted strain. We appreciate the comment raised anonymously by a reader, presumably a virologist, who pointed us to the difference between the vaccine strain and laboratory-adapted strain.

The aim of our study (Takaki et al., 2011) was to clarify the pathway of IFN induction in MV strains with different sequences. I believe that the reader and I agreed that the C272R mutation of MV V protein fails to block MDA5 and thereby up-regulates type I IFN induction. This C272R strain appeared to be derived from the ED strain with V protein mutation (Combredet et al., 2003). The V protein mutation may tend to occur in ED laboratory-adapted strains through adaptation to Vero cells which lack antiviral type I IFN response. Ohno et al. (2004) first provided the data on V protein mutation facilitating IFN alpha-dependent IFN-signaling in a MV strain of a C272R mutant, named Edtag. This means that Edtag C272R mutation releases the block of the IFNAR-STAT1/2/IRF-9 pathway by MV V protein, allowing IFN-alpha amplification (Taniguchi and Takaoka, 2002). On the other hand, Takaki's report here (Takaki et al., 2011) indicates that failure of the C272R mutant to sufficiently block MV-mediated IFN induction is rooted in the uncontrolled IPS-1 pathway, which leads to enhanced IRF-3 nuclear translocation.

Shingai et al. (2007) previously reported that defective interference (DI) RNA produced in MV-replicating cells causes accelerated MV-mediated induction of type I IFN. DI RNA acts on the cytoplasmic sensors, RIG-I/MDA5, leading to activation of the IPS-1 pathway (Yoneyama and Fujita, 2007) Studies by Ohno and Shingai revealed that MV laboratory-adapted strains could up-regulate IFN induction in affected cells by two distinct modes: V protein mutation (Ohno et al., 2004) and production of DI RNA (Shingai et al., 2007). Takaki's data (Takaki et al., 2011) further demonstrated that both modes of C272R mutation and DI RNA production involve the IPS-1 pathway, not only the IFNAR pathway. This is just the conclusion this paper wanted to emphasize.

Takaki's results were recently confirmed in a report by Haralambieva et al. (2010). The main conclusion of our study is thus confirmed in both innate immunity and virology laboratories. We think this is a good example of how progress in the field of viral immunity will be attained by promoting communication between the fields of virology and innate immunology.

Correction

Abstract near to the last conclusion: the structural difference of laboratory-adapted MV V protein hampers MDA5 blockade and acts as a nidus for the spread/amplification of type I IFN induction.

DOI of original article: 10.1016/j.molimm.2010.10.006.
Tel.: +81 11 706 5073; fax: +81 11 706 7866.
E-mail address: seya-tu@pop.med.hokudai.ac.jp

0161-5890/$ – see front matter
doi: 10.1016/j.molimm.2011.04.007

References

Combredet, C., Labrousse, V., Mollet, L., Lorin, C., Delebecque, F., Hurtrel, B., McClure, H., Feinberg, M.B., Brahic, M., Tangy, F., 2003. A molecularly cloned Schwarz strain of measles virus vaccine induces strong immune responses in macaques and transgenic mice. J. Virol. 77, 11546–11554.

Haralambieva, I.H., Ovsyannikova, I.G., Dhiman, N., Vierkant, R.A., Jacobson, R.M., Poland, G.A., 2010. Differential cellular immune responses to wild-type and attenuated Edmonston tag measles virus strains are primarily defined by the viral phosphoprotein gene. J. Med. Virol. 82, 1966–1975.

Ohno, S., Ono, N., Takeda, M., Takeuchi, K., Yanagi, Y., 2004. Dissection of measles virus V protein in relation to its ability to block alpha/beta interferon signal transduction. J. Gen. Virol. 85, 2991–2999.

Parks, C.L., Lerch, R.A., Walpita, P., Wang, H.P., Sidhu, M.S., Udem, S.A., 2001. Comparison of predicted amino acid sequences of measles virus strains in the Edmonston vaccine lineage. J. Virol. 75, 910–920.

Shingai, M., Ebihara, T., Begum, N.A., Kato, A., Honma, T., Matsumoto, K., Saito, H., Ogura, H., Matsumoto, M., Seya, T., 2007. Differential type I IFN-inducing abilities of wild-type versus vaccine strains of measles virus. J. Immunol. 179, 6123–6133.

Takaki, H., Watanabe, Y., Shingai, M., Oshiumi, H., Matsumoto, M., Seya, T., 2011. Strain-to-strain difference of V protein of measles virus affects MDA5-mediated IFN- -inducing potential. Mol. Immunol. 48, 497–504.

Taniguchi, T., Takaoka, A., 2002. The interferon-alpha/beta system in antiviral responses: a multimodal machinery of gene regulation by the IRF family of transcription factors. Curr. Opin. Immunol. 14, 111–116.

Yoneyama, M., Fujita, T., 2007. RIG-I family RNA helicases: cytoplasmic sensor for antiviral innate immunity. Cytokine Growth Factor Rev. 18, 545–551.

The TLR3/TICAM-1 Pathway Is Mandatory for Innate Immune Responses to Poliovirus Infection

Hiroyuki Oshiumi,*,[1] Masaaki Okamoto,*,[1] Ken Fujii,[†] Takashi Kawanishi,* Misako Matsumoto,* Satoshi Koike,[†] and Tsukasa Seya*

Cytoplasmic and endosomal RNA sensors recognize RNA virus infection and signals to protect host cells by inducing type I IFN. The cytoplasmic RNA sensors, retinoic acid inducible gene I/melanoma differentiation-associated gene 5, actually play pivotal roles in sensing virus replication. IFN-β promoter stimulator-1 (IPS-1) is their common adaptor for IFN-inducing signaling. Toll/IL-1R homology domain-containing adaptor molecule 1 (TICAM-1), also known as TRIF, is the adaptor for TLR3 that recognizes viral dsRNA in the early endosome in dendritic cells and macrophages. Poliovirus (PV) belongs to the Picornaviridae, and melanoma differentiation-associated gene 5 reportedly detects replication of picornaviruses, leading to the induction of type I IFN. In this study, we present evidence that the TLR3/TICAM-1 pathway governs IFN induction and host protection against PV infection. Using human PVR transgenic (PVRtg) mice, as well as IPS-1$^{2/2}$ and TICAM-1$^{2/2}$ mice, we found that TICAM-1 is essential for antiviral responses that suppress PV infection. TICAM-1$^{2/2}$ mice in the PVRtg background became markedly susceptible to PV, and their survival rates were decreased compared with wild-type or IPS-1$^{2/2}$ mice. Similarly, serum and organ IFN levels were markedly reduced in TICAM-1$^{2/2}$/PVRtg mice, particularly in the spleen and spinal cord. The sources of type I IFN were CD8a^{+}/CD11c^{+} splenic dendritic cells and macrophages, where the TICAM-1 pathway was more crucial for PV-derived IFN induction than was the IPS-1 pathway in ex vivo and in vitro analyses. These data indicate that the TLR3/TICAM-1 pathway functions are dominant in host protection and innate immune responses against PV infection. The Journal of Immunology, 2011, 187: 5320–5327.

When RNA viruses infect mammalian cells, type I IFN is generated to suppress viral infection. IFN-inducing pathways evoked by viral dsRNA have been identified in humans and mice, and the possible involvement of these pathways in protection against viruses has been examined using gene-disrupted mice and various virus species (1). The sensing of dsRNA by the innate immune system is accomplished either by TLR3 or by cytoplasmic sensors such as dsRNA-dependent protein kinase (so-called PKR), retinoic acid inducible gene I (RIG-I), and melanoma differentiation-associated gene 5 (MDA5) (2). In virus-infected cells, RIG-I and MDA5 mainly participate in type I IFN induction in conjunction with the adaptor molecule IFN-β promoter stimulator-1 (IPS-1; also known as MAVS, Cardif, or VISA) (1). The role of these molecules in host cell protection has been clearly delineated in RNA virus infection.

Toll/IL-1R homology domain-containing adaptor molecule 1 (TICAM-1; also called TRIF) is the adaptor of TLR3 (3–5). When TLR3 senses dsRNA on the endosomal membrane, it induces type I IFN (6, 7). The adaptor TICAM-1 plays a pivotal role in TLR3-mediated IFN-α/β induction. Once dsRNA stimulates TLR3, TICAM-1 transiently couples with TLR3 and forms a multimer, translocating to a distinct region of the cytoplasm (8). In its multimeric form, TICAM-1 recruits the kinase complex to activate IFN regulatory factors (IRF)-3 and -7, which induce type I IFN production (7, 9). Historically, this IFN-inducing pathway was identified earlier than the cytoplasmic RIG-I/MDA5 pathway (10, 11). Many reports have mentioned the possibility that the TLR3/TICAM-1 pathway is involved in the anti-viral IFN response (12), but no definitive evidence of the anti-viral properties of this pathway has been obtained using TICAM-1$^{2/2}$ mice (13). Only a DNA virus, mouse CMV (MCMV), has been shown to infect TICAM-1$^{2/2}$ mice, and thus mouse cells are partly protected from MCMV by the TICAM-1 pathway (5, 14).

Poliovirus (PV) is a positive strand ssRNA virus that produces dsRNA intermediates during viral replication (15), modified with 5′ terminal Vpg protein (16), a characteristic feature of picornaviruses. It is generally accepted that picornaviruses are recognized by MDA5 but not RIG-I in infected cells, presumably due to the generation of this unusual dsRNA. This concept was confirmed by the finding that MDA5$^{2/2}$ mice fail to induce type I IFN in response to encephalomyocarditis virus (EMCV) and permit severe EMCV infection (13, 17). However, another picornavirus, coxsackie B virus (CBV) serotype 3, is recognized by TLR3 in infected cells and induces IFN-γ as an effector for suppressing CBV infection

*Department of Microbiology and Immunology, Hokkaido University Graduate School of Medicine, Sapporo 060-8638, Japan; and [†]Department of Microbiology and Immunology, Tokyo Metropolitan Institute for Neuroscience, Tokyo Metropolitan Organization for Medical Research, Tokyo 156-0057, Japan

[1]H.O. and M.O. contributed equally to this work.

Received for publication May 24, 2011. Accepted for publication September 6, 2011.

This work was supported in part by Grants-in-Aid from the Ministry of Education, Science, and Culture of Japan (Specified Project for Advanced Research), the Ministry of Health, Labor, and Welfare of Japan, the Takeda Foundation, and by the Waxmann Foundation. Financial support by the Program of Founding Research Centers for Emerging and Reemerging Infectious Diseases, Ministry of Education, Culture, Sports, Science, and Technology of Japan, is gratefully acknowledged.

Address correspondence and reprint requests to Prof. Tsukasa Seya, Department of Microbiology and Immunology, Graduate School of Medicine, Hokkaido University, Kita-ku, Kita-15 Nishi-17, Sapporo, Hokkaido 060-8638, Japan. E-mail address: seya-tu@pop.med.hokudai.ac.jp

The online version of this article contains supplemental material.

Abbreviations used in this article: BM, bone marrow; BM-DC, bone marrow-derived dendritic cell; BM-Mf, bone marrow-derived macrophage; CBV, coxsackie B virus; DC, dendritic cell; EMCV, encephalomyocarditis virus; HCV, hepatitis C virus; IFIT-1, IFN-induced protein with tetratripeptide repeats 1; IP-10, IFN-γ–induced protein 10; IPS-1, IFN-β promoter stimulator-1; IRF, IFN regulatory factor; KO, knockout; MCMV, mouse cytomegalovirus; MDA5, melanoma differentiation-associated gene 5; MEF, mouse embryonic fibroblast; Mf, macrophage; MOI, multiplicity of infection; PV, poliovirus; PVRtg, poliovirus receptor transgenic; RIG-I, retinoic acid inducible gene I; RT-qPCR, real-time quantitative PCR; TICAM-1, Toll/IL-1R homology domain-containing adaptor molecule 1; WNV, West Nile virus; WT, wild-type.

www.jimmunol.org/cgi/doi/10.4049/jimmunol.1101503

(18). In this study, we analyzed in vivo infection of a popular picornavirus, PV, using PVR transgenic (PVRtg) mice, which show a neurotropic phenotype during PV infection similar to humans (19, 20). Using this mouse model, in combination with TICAM-1$^{2/2}$ or IPS-1$^{2/2}$ mice, we present evidence that the host TICAM-1 pathway, particularly in macrophages (Mf), serves as a source of type I IFN induction and protects host PVRtg mice from PV infection and paralytic death. Thus, the strategy for host protection against picornaviruses is not simply based on the MDA5-dependent dsRNA recognition, but is variable depending on picornavirus species.

Materials and Methods

Mice

All mice were backcrossed with C57BL/6 mice more than seven times before use. TICAM-1$^{2/2}$ (21) and IPS-1$^{2/2}$ mice (this study) were generated in our laboratory. TLR3$^{2/2}$ (4), IRF-3$^{2/2}$, and IRF-7$^{2/2}$ mice (22) were provided by Drs. S. Akira (Osaka University, Osaka, Japan) and T. Taniguchi (University of Tokyo, Tokyo, Japan). PVRtg mice were provided as reported previously (20). All mice were maintained under specific pathogen-free conditions in the Animal Facility at Hokkaido University Graduate School of Medicine (Sapporo, Japan). Animal experiments were performed according to the guidelines set by the Animal Safety Center, Japan.

Generation of IPS-1–deficient mice

The IPS-1 gene was amplified by PCR using genomic DNA extracted from embryonic stem cells. The targeting vector was constructed by replacing the second and third exons with a neomycin-resistance gene cassette (Neo), and an HSV thymidine kinase driven by the PGK promoter was inserted into the genomic fragment for negative selection. After the targeting vector was transfected into 129/Sv mice-derived embryonic stem cells, G418 and ganciclovir doubly resistant colonies were selected and screened by PCR. The targeted cell line was injected into C57BL/6 blastocysts, resulting in the birth of male chimeric mice. These mice were then backcrossed with C57BL/6 mice. The disruption of the IPS-1 gene was confirmed by PCR for the long and short arms. The abolishment of IPS-1 mRNA expression was confirmed by real-time quantitative PCR (RT-qPCR).

Cells, viruses, and reagents

Wild-type (WT) and TICAM-1$^{2/2}$ mouse embryonic fibroblasts (MEF) were prepared from 12.5- to 13.5-d-old embryos. PV, strain Mahoney, was amplified in Vero cells, and the viral titer was determined by a plaque assay. Bone marrow (BM) cells were prepared from the femur and tibia. The cells were cultured in RPMI 1640 (Invitrogen, New York, NY) supplemented with 10% FCS, 100 mM 2-ME, and 10 ng/ml murine GM-CSF or the culture supernatant of NIH3T3 cells expressing M-CSF. After 6 d, cells were collected and used as bone marrow-derived dendritic cells (BM-DC) or BM-derived macrophages (BM-Mf). For the preparation of BM-DC and BM-Mf, the medium was changed every 2 d. Splenic DC and NK cells were isolated using the MACS system (Miltenyi Biotec, Auburn, CA).

Experimental infection of mice

Five- to 8-wk-old C57BL/6 female mice were used throughout this study. Mice of different genotypes were i.p. or i.v. infected with PV at the doses indicated. The viability of the infected mice was monitored for 2 wk. We collected sera from the mice at different time points to measure viral titers by a plaque assay and cytokine levels by an ELISA. To determine the tissue viral titer, mice were euthanized and organs were aseptically removed and frozen by liquid nitrogen. Because the organs were not perfused before organs were removed, virus titers were determined including blood. Specimens were homogenized in 2 ml PBS on ice, and titers were determined by a plaque assay.

ELISA

Culture supernatants of cells (10^5) seeded on 24-well plates or sera were collected and analyzed for cytokine levels with ELISA. ELISA kits for IFN-a and IFN-b were purchased from PBL Biomedical Laboratories. ELISA was performed according to the manufacturer's instructions.

qPCR

For qPCR, total RNA was extracted with TRIzol (Invitrogen), and 0.2–0.5 mg RNA was reverse-transcribed using a high-capacity cDNA transcription kit (Applied Biosystems, Piscataway, NJ) with random primers according to the manufacturer's instructions. qPCR was performed using a Step One real-time PCR system (Applied Biosystems).

In vivo blocking of NK activity

Mice (PVRtg and PVRtg/TICAM-1$^{2/2}$) were i.p. injected with 250 mg anti-NK1.1 Ab, asialoGM1 Ab, or control PBS as described previously (21). One day later, the mice were i.p. inoculated with 10^4 PFU PV. One to 7 d after PV injection, depletion of peripheral NK1.1$^+$ cells was confirmed by flow cytometry. Then, the mortality of the mice was monitored. In some experiments, the spleen cells were harvested and NK cells (DX5$^+$ cells) were positively isolated using the MACS system (Miltenyi Biotec). The DX5$^+$ NK cells were suspended in RPMI 1640 containing 10% FCS and mixed with ^{51}Cr-labeled B16D8 cells at the indicated E:T ratios. After 4 h, the supernatants were harvested and [^{51}Cr] release was measured.

Statistical analysis

Statistical significance of differences between groups was determined by the Student t test, and survival curves were analyzed by the log-rank test using Prism 4 for Macintosh software (GraphPad Software). Student t tests and x^2 goodness-of-fit tests were performed using Microsoft Excel software and a x^2 distribution table.

Results

TICAM-1 is essential for protection of PVRtg mice against PV infection

Mice lacking the mda-5 gene abrogate the production of type I IFN in response to EMCV infection and are more susceptible to infection with EMCV (13, 17). Because EMCV is a picornavirus, it has been proposed that MDA5 is critical for sensing picornavirus infection. In infected cells, picornaviruses efficiently generate long dsRNA, which is recognized by the cytoplasmic dsRNA sensor MDA5 (23). The 5′ end of the PV genomic RNA is linked to a VPg protein (16), not to a 5′-triphosphate, a major ligand for another cytoplasmic RNA sensor, RIG-I (24, 25). Thus, we first tested, using the PVRtg mouse model (20), whether the mortality of PV-infected mice is affected by disruption of IPS-1 (Fig. 1A). Approximately 70% of WT (PVRtg) mice and 40% of IPS-1$^{2/2}$ mice survived . 10 d postinoculation at an i.p. dose of 2 3 10^4 PFU. No statistical significance between these two groups was detected (Fig. 1A). In the same experiments, TICAM-1$^{2/2}$ mice died within 5 d by paralysis (Fig. 1B).

We next investigated the effect of the route of PV infection on mortality in this mouse model. PV (2 3 10^3 PFU) was injected i.p. or i.v. into WT and TICAM-1 mice and their mortality was examined (Fig. 1C, 1D). All TICAM-1$^{2/2}$ mice died by paralysis within 7.5 d irrespective of the injection route. The significance of this early mortality rate of PV-infected TICAM-1$^{2/2}$ mice was supported by statistical analysis. The mortality rates were slightly high in WT mice compared with IPS-1$^{2/2}$ mice when PV loads in mice were not very high (Supplemental Fig. 1A). This tendency seemingly diminished by early death of IPS-1$^{2/2}$ mice with high doses of PV input. These data suggested that TICAM-1, rather than IPS-1 (or the sensors RIG-I and MDA5), is a critical factor in protecting mice from PV-mediated paralytic death. This conclusion was confirmed using RIG-I$^{2/2}$ and MDA5$^{2/2}$ mice with a PVRtg background (S. Abe, K. Fujii, and S. Koike, submitted for publication).

These results showed a discrepancy with previous indications that MDA5 is critical in picornavirus protection (13). We therefore tested the dose dependence of PV in the survival of WT versus TICAM-1$^{2/2}$ mice. Surprisingly, high doses of PV (2 3 10^5 and 2 3 10^6 PFU) induced paralytic death in all WT as well as TICAM-1$^{2/2}$ mice within 6 d (Fig. 2A, 2B). Thus, high doses of PV (. 2 3 10^5 PFU) appear to overpower the TICAM-1 PV-protective activity in vivo, which confirmed previous findings using other picornaviruses (13). TICAM-1 was most effective in

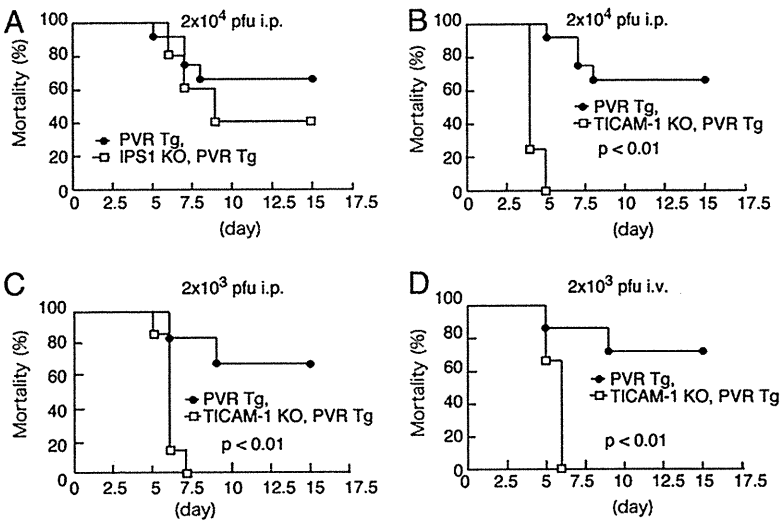

FIGURE 1. Survival of WT, TICAM-1 KO, and IPS-1 KO mice following i.p. or i.v. PV infection. A and B, PV (2 3 10^4 PFU) was infected via the i.p. route into WT and IPS-1 (A) or TICAM-1 (B) KO mice (n $ 5), and survival was monitored for 14 d. C and D, PV (2 3 10^3 PFU) was infected via the i.p. (C) or i.v. (D) route into WT and TICAM-1 KO mice (n $ 5), and survival was monitored for 14 d.

the survival against PV infection at low dose (, 2 3 10^4 PFU) (Figs. 1B, 1C, 2C). Similar results were obtained with the PV infection study (S. Abe, K. Fujii, and S. Koike, submitted for publication) when TICAM-$1^{2/2}$ mice were substituted with TLR$3^{2/2}$ or IRF-3/7 double-knockout (KO) mice. Results were confirmed using IRF-$3^{2/2}$ and IRF-$7^{2/2}$ mice (26). These results are essentially consistent with previous reports using a PVRtg/IFNAR$^{2/2}$ mouse model (27), in which type I IFN is critical for PV permissiveness, particularly in the intestine of PVRtg mice.

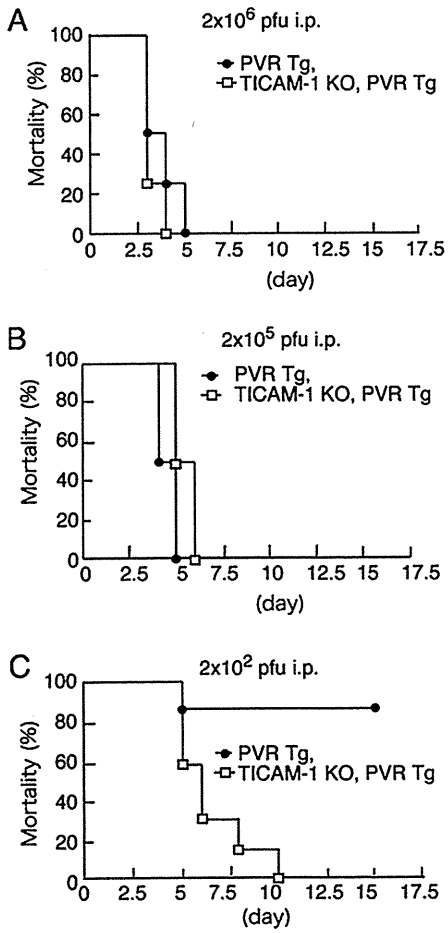

FIGURE 2. High doses of PV disable the protective effect of TICAM-1. WT and TICAM-1 KO mice (n $ 6) were i.p. infected with 2 3 10^6 (A), 2 3 10^5 (B), or 2 3 10^2 PFU (C) PV and survival was monitored for 14 d.

TICAM-1–dependent type I IFN induction in PVRtg mice

PV titers in various organs were measured with WT and TICAM-$1^{2/2}$ mice i.p. injected with 2 3 10^4 PFU PV. In most organs, PV titers were higher in TICAM-$1^{2/2}$ mice than in WT mice at day 3 post-infection (Fig. 3A). The PV titer ratio in TICAM-$1^{2/2}$ versus WT mice was also high in the lung (Fig. 3A). In most organs except for the large intestine, high PV titers were harvested in TICAM-$1^{2/2}$ mice compared with WT mice. The difference in local PV titers between WT and TICAM-$1^{2/2}$ mice was culminated in the lung and spinal cord (Fig. 3A). Serum PV titers were increased within 48 h

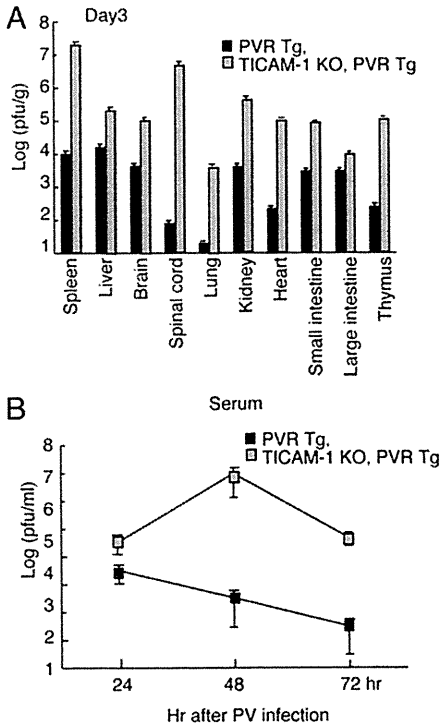

FIGURE 3. Viral titers in organs and serum following PV infection. WT and TICAM-1 KO mice were infected i.p. with 2 3 10^4 PFU PV. The viral titers in each organ (A) and sera (B) were measured by a plaque assay. Data are shown as means 6 SD of three independent samples.

after PV i.p. injection in TICAM-1$^{2/2}$ mice compared with WT mice (Fig. 3B).

IFN-a/b levels were measured with sera from WT, IPS-1$^{2/2}$, and TICAM-1$^{2/2}$ mice, but they were barely detected in these PV-infected mice (Supplemental Fig. 1B). Only i.v. injection of high PV titers (an example shows . 4 3 10^6 PFU) allowed WT mice to release type I IFN within 12 h (Supplemental Fig. 1B). No IFN was detected in blood in TICAM-1$^{2/2}$ and IPS-1$^{2/2}$ mice even in this high-dose setting. However, IFN-a production was reproduced in a cell type level (peritoneal Mf) in vitro (Supplemental Fig. 1C). PV infection-mediated cell death (28) and degradation of MDA5 protein (29) may be major causes for this undetectable type I IFN production during in vivo PV infection.

TICAM-1 pathway contributes to IFN-b induction in WT mice with low PV titers

We next determined the mRNA levels of type I IFN in each organ extracted from PV (2 3 10^4 PFU)-infected WT and TICAM-1$^{2/2}$ mice. IFN-b mRNA was upregulated in all of the organs tested in WT mice within 12 h in response to PV injection (i.p.) (Fig. 4A). In contrast, only a low increase in IFN-b mRNA was detected in the organs of TICAM-1$^{2/2}$ mice (Fig. 4A). IFN-a2 mRNA was upregulated in the organs of TICAM-1$^{2/2}$ and WT mice to similar extents in response to PV injection (2 3 10^4 PFU, i.p.) (Fig. 4B). Notable decreases in IFN-a2 mRNA were observed in the TICAM-1$^{2/2}$ spleen and spinal cord compared with WT controls (Fig. 4B). The mRNA levels of genes associated with type I IFN induction were evaluated by qPCR, and no unique differences were observed between the splenocytes from PV-injected TICAM-1$^{2/2}$ and IPS-1$^{2/2}$ mice (Supplemental Fig. 1D). Hence, type I IFN mRNA is generally upregulated via TICAM-1 in the local organs of PVRtg WT mice during PV infection.

The mRNA levels of IFN-inducible genes and other cytokines were determined in spleen cells after PV infection. IFN-l and IFN-g–induced protein 10 (IP-10) mRNA were upregulated in the spleen cells of WT, but not TICAM-1$^{2/2}$ mice, after PV infection (multiplicity of infection [MOI] of 1) (Fig. 4C), with profiles similar to that of IFN-b mRNA (Fig. 4C). A sensor for 5′-triphosphorylated RNA, IFN-induced protein with tetratripeptide repeats 1 (IFIT-1), was also upregulated through PV infection (Fig. 4C). TNF-a, IL-10, IL-12p40, and IFN-g, which may be associated with infectious cell death, were barely upregulated in spleen cells in response to PV infection (Supplemental Fig. 1E).

TICAM-1–dependent type I IFN induction by PV depends on Mf in PVRtg mice

The types of cells that participate in type I IFN induction in the spleen were examined by sorting spleen cells. IFN-b and IFN-a2 were found to be induced in WT CD11c$^+$ DC (Fig. 5A), whereas CD11c^2 cells barely induced type I IFN. Furthermore, IFN-b and IFN-a2 were barely induced in TICAM-1$^{2/2}$ CD11c$^+$ cells (Fig. 5B). Participation of IPS-1 in type I IFN induction in CD11c$^+$ myeloid cells is less compared with that of TICAM-1 (Fig. 5B).

Splenic CD8a$^+$CD11c$^+$ and CD4$^+$CD11c$^+$ cells were separated by MACS beads and their response to PV (MOI of 1) was analyzed by determining the mRNA levels of type I IFN (Fig. 5C). CD8a$^+$CD11c$^+$ cells, but not the CD4$^+$CD11c$^+$ cells, of WT mice were responsible for type I IFN induction by PV. There was a CD4^{2}CD8a^2 population of DC in the spleen and this type of cells did not induce type I IFN in response to PV (Supplemental Fig. 2). The generation of the mRNA of type I IFN and IFIT-1 by PV infection was abrogated in the TICAM-1$^{2/2}$ CD8a$^+$CD11c$^+$ splenic DC (Fig. 5D). Also, CD4/8a double-negative DC failed to express type I IFNs (Supplemental Fig. 2). Thus, CD8a$^+$CD11c$^+$ DC, which reportedly express TLR3 (30), are the source of type I IFN in PV-infected PVRtg mice.

We finally confirmed that type I IFN is locally induced in TLR3$^+$ myeloid cells during PV infection. BM-Mf and BM-DC were prepared from mouse BM and challenged with PV (MOI of 1). These cells express TLR3 in the endosome as previously reported about mouse BM-DC (30) and human monocyte-derived DC (31). BM-Mf showed similar profiles of type I IFN mRNA to those of PV-infected splenocytes (Figs. 4C, 6A). However, IFN-l and IP-10 mRNA were not detectable in PV-infected BM-Mf, the reason for which remains unclear (Fig. 6A). IL-12p40, a representative TICAM-1–dependent gene, was transiently upregulated

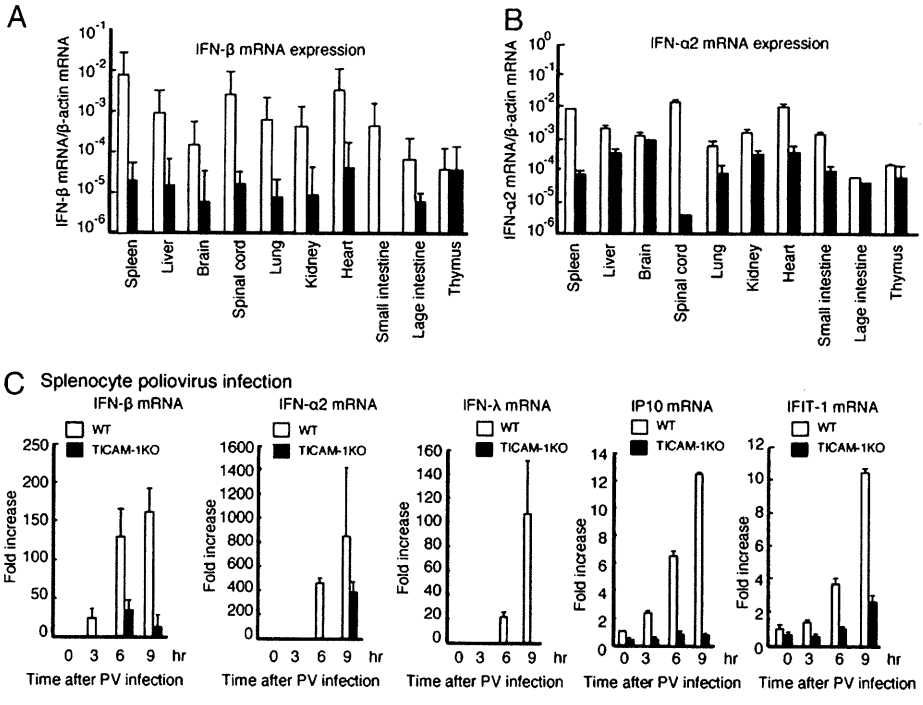

FIGURE 4. The expression of type I IFN following PV infection. A and B, WT and TICAM-1 KO mice were infected i.p. with 2 3 10^4 PFU PV. Three days postinfection, the mRNA expression levels of IFN-b (A) and IFN-a (B, C) were determined by RT-qPCR. C, Splenocytes (5 3 10^5) were infected with PV (MOI of 1) and the mRNA expression levels of IFN-b, IFN-a2, IFN-l, IP-10, and IFIT-1 were measured by RT-qPCR. Data are shown as means 6 SD and are representative of three independent experiments.

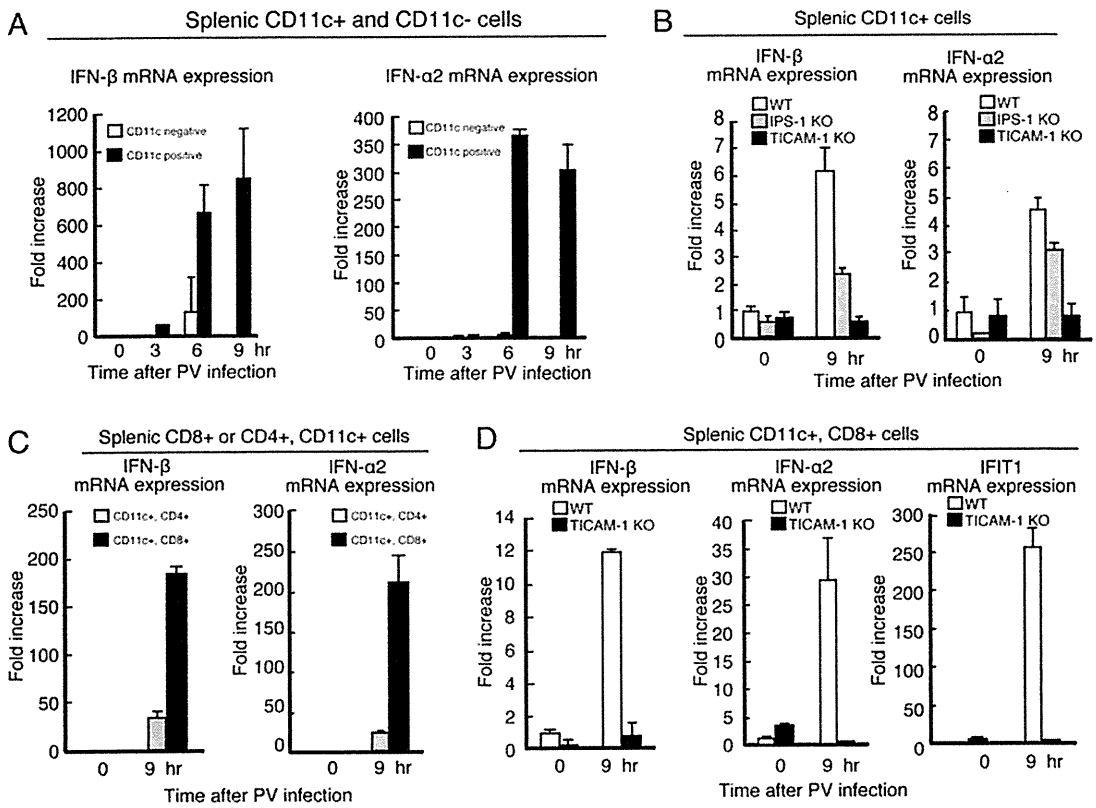

FIGURE 5. The expression of type I IFN in splenic DC. A, were isolated from WT spleens using the MACS system. CD11c$^+$ or CD11c^2 cells (5 3 10^5) were infected with PV (MOI of 1), and the mRNA expression of type I IFNs was measured by RT-qPCR. B, WT, TICAM-1, and IPS-1 knockout splenic CD11c$^+$ cells were infected with PV, and the expression of type I IFNs was measured by RT-qPCR. C, CD8a$^+$CD11c$^+$ cells and CD4$^+$CD11c$^+$ cells were isolated from WT spleens and infected with PV (MOI of 1). The expression of type I IFNs was measured by RT-qPCR. D, CD8a$^+$CD11c$^+$ splenic cells were isolated from WT and TICAM-1 KO mice and infected with PV (MOI of 1). The expressions of type I IFNs and IFIT-1 were measured by RT-qPCR. Data are shown as means 6 SD and are representative of three independent experiments.

in BM-Mf 4 h after PV infection (Supplemental Fig. 3). Similarly, but less prominently, the profiles of type I IFN and IL-12p40 were observed in BM-DC (Fig. 6A, Supplemental Fig. 3) and CD11c$^+$CD8$^+$ splenic DC (Fig. 5D). Therefore, taken together, these results indicate that IL-12 and IFN-a/b are only minimally upregulated in splenic DC in a PV-dependent manner.

The production of IFN-a was determined by ELISA in the supernatant of PV-infected BM-Mf and BM-DC (Fig. 6C). BM-Mf prepared from WT mice generated higher amounts of IFN-a than did those from TICAM-1$^{2/2}$ mice. Although similar results were obtained with BM-DC, the effect of TICAM-1 depletion was not statistically significant (Fig. 6C).

NK cells and MEF do not play major roles in protection against PV infection

Using NK1.1-depleted mice, we tested the possible participation of NK cells in the protection of PVRtg mice from PV infection (Fig. 7). NK1.1$^+$ cells were depleted from mouse blood 1 d after injection (i.p.) of NK1.1 Ab into WT (Fig. 7A) and TICAM-1$^{2/2}$ mice. After PV challenge, WT mice inoculated with control saline and NK1.1 Ab survived similarly, whereas TICAM-1$^{2/2}$ mice were all killed by PV within 7.5 d irrespective of NK1.1 pretreatment (Fig. 7B). Hence, NK cell activation does not affect PV-derived death. The lack of TICAM-1 was also found to have no effect on the NK cell-mediated rescue of PV-infected mice.

Mouse fibroblasts are known to be a potential source of type I IFN (13). We therefore checked whether MEF induce type I IFN and protection against PV (Supplemental Fig. 4). MEF from WT PVRtg mice were susceptible to PV, with cell death being observed at an MOI of 1. MEF from TICAM-1$^{2/2}$ PVRtg mice were 1 log more susceptible to PV, with cell death occurring at an MOI of 0.1 (Supplemental Fig. 4A). IFN-b was upregulated in PV-infected MEF to only a slightly higher level in PVRtg MEF than in TICAM-1$^{2/2}$ PVRtg MEF (Supplemental Fig. 4B). These results suggested that the large difference in the PV survival rate between WT and TICAM-1$^{2/2}$ mice is not caused by NK cells or type I IFN induction by fibroblasts. The TICAM-1 pathway plays a key role for producing IFN-a/b in Mf/DC, but not in fibroblasts, during PV infection in PVRtg mice.

Discussion

In this study, we demonstrated that PV infection is exacerbated in TICAM-1$^{2/2}$ PVRtg mice. There are a number of RNA-sensing molecules that serve as anti-virus agents and function in a cell type-specific manner. Based on trials using gene-disrupted mice and human viruses, RIG-I has been reported to be essential for sensing infection by rhabdoviruses, influenza viruses, paramyxoviruses, and flaviviruses, whereas MDA5 is important for sensing picornavirus infection (13, 33). In previous studies on picornaviruses, however, only EMCV and several species of picornaviruses have been employed for the KO mice analyses (13). The essential role of type I IFN in PV tropism has been well characterized in PVRtg mice (34). To our knowledge, this study is the first to investigate the sensor that detects PV infection in PVRtg PV-sensitive mice. Because RIG-I and MDA5 use the adaptor IPS-1, we constructed an IPS-1$^{2/2}$ mouse strain for this

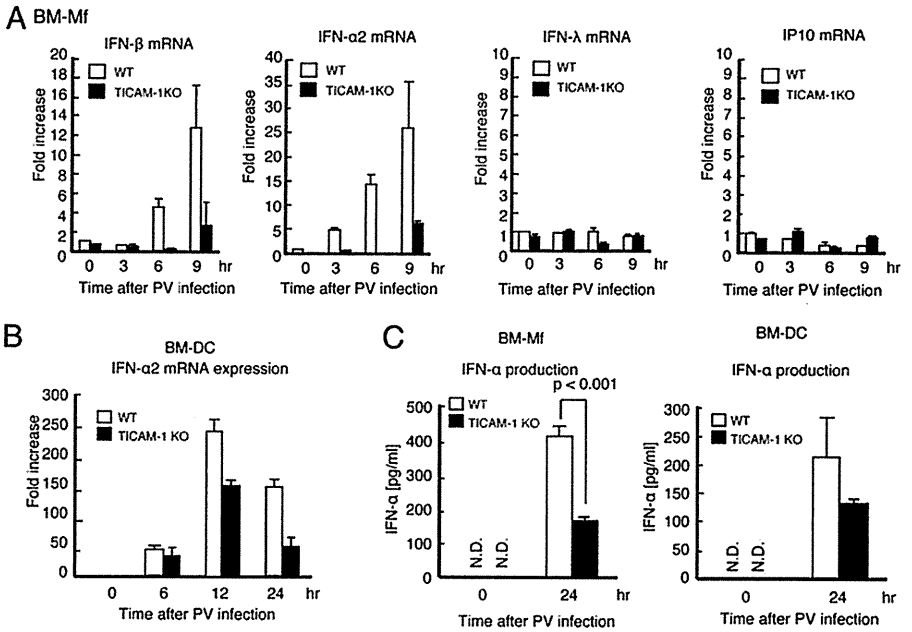

FIGURE 6. Production of type I IFN from BM-Mf and BM-DC. BM-Mf (A) and BM-DC (B) were prepared from BM cells with M-CSF and GM-CSF, respectively (32). The cells were infected with PV (MOI of 1), and the expression levels of IFN-b, IFN-a2, IFN-l, and IP-10 were determined by RT-qPCR. C, IFN-a produced by PV-infected BM-Mf and BM-DC was measured by ELISA. BM-Mf and BM-DC were prepared from BM cells of WT and TICAM-1 $^{2/2}$ mice as in A and B. Data are shown as means 6 SD and are representative of three independent experiments.

study. Unexpectedly, however, IPS-1 was dispensable for protection against PV infection in vivo. This study, taken together with other reports (33, 35, 36), suggests that each virus species has its own strategy to evade host immune attack. This is true even in picornavirus subspecies. Although the IPS-1 pathway involving RIG-I and MDA5 is important for sensing and preventing cytoplasmic virus replication, other steps also participate in critical regulation of virus replication. PV infection is the case where MDA5 is not absolutely critical, but TICAM-1 is essential, for virus protection.

The TICAM-1 pathway participates in driving NK/CTL activation in DC/Mf (21, 37). This pathway is involved in type I IFN induction, as in the IPS-1 pathway, but cells expressing TLR3 are limited. The TLR3 distribution profile by flow cytometry confirms its expression in myeloid cells in mice (30). The TICAM-1 pathway converges with the IPS-1 pathway via the molecular complex of IRF-3–activating kinases (38), and therefore activation of the TICAM-1 pathway induces type I IFN and other IFN-inducible genes (39). Nevertheless, gene induction profiles differ between the TICAM-1 and IPS-1 pathways (40), which may explain the functional distinction between the sensor that is triggered in the virus-infected cells (MDA5/IPS-1) and the sensor that is required for DC/Mf to mount immune responses. Studying these gene functions will be an important issue for functional discrimination between the intrinsic versus extrinsic sensors.

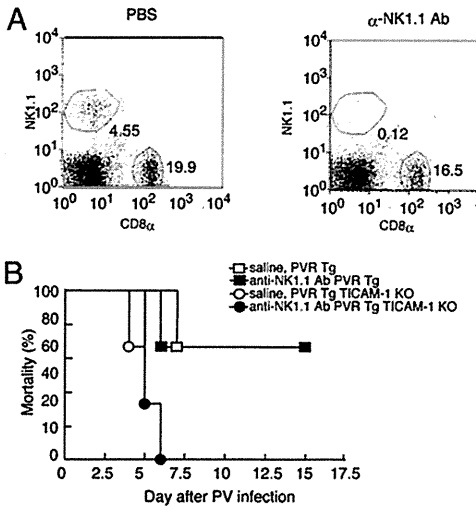

FIGURE 7. Effect of NK cells on mortality of PV-infected TICAM-1 $^{2/2}$ PVRtg mice. A, To block the NK cell activity in mice, NK1.1 Ab or PBS (control) was i.p. injected into WT mice (n $ 6). After 24 h, spleen cells were isolated from the mice and the fraction of NK1.1$^+$ cells was measured by FACS analysis. B, NK1.1 Ab or PBS was i.p. injected into WT and TICAM-1 KO mice. After 24 h, the mice were infected i.p. with PV, and survival was monitored for 15 d.

RIG-1/MDA5 are distributed over almost all organs, including Mf/DC. An interesting point concerns what the function is of the IPS-1 pathway in Mf/DC. Without conditional KO mice, we have an experimental limit to discriminate between their intrinsic function that is triggered in PV-infected cells and the extrinsic function leading Mf/DC to driving the innate immune response. Because the TLR3/TICAM-1 pathway is conserved in Mf/DC, the CNS, fibroblasts, and epithelical cells, it is reasonable that their functions are rather specified in Mf/DC and the neuronal system in PV infection.

However, except several examples such as rhabdovirus (41) and hepatitis C virus (HCV) (32), no definitive evidence has been reported supporting the role of TLR3/TICAM-1 in anti-RNA virus function using KO mice, unlike IPS-1 (35, 36). In previous studies, we used RNA viruses and their mouse models of measles virus, respiratory syncitial virus, vesicular stomatitis virus, influenza virus, and rotavirus infection (12), but we were unable to demonstrate solid antiviral function of the TLR3/TICAM-1 pathway in these models (12). Accordingly, which type I IFN, IFN-inducible gene, NK cell, or CTL is an effector for antagonizing viral replication still remains uncharacterized. To our knowledge, the results of our present study first demonstrated that the TLR3/TICAM-1 pathway is indispensable for induction of the type I IFN effector, but not NK cell activation, which is a critical event in the elimination of virus-infected cells and host protection against PV. IL-12 and IFN-g are not upregulated in splenic DC in a PV-dependent manner. Furthermore, CTL are unlikely to be involved in our present model, since they would not function within the time scale of several days after initial infection (42).